Contents

Musical Instrument Sound Conversion

- Demonstration: Learn from a system (Piano sound) and transfer the knowledge for a new system (Guitar sound)

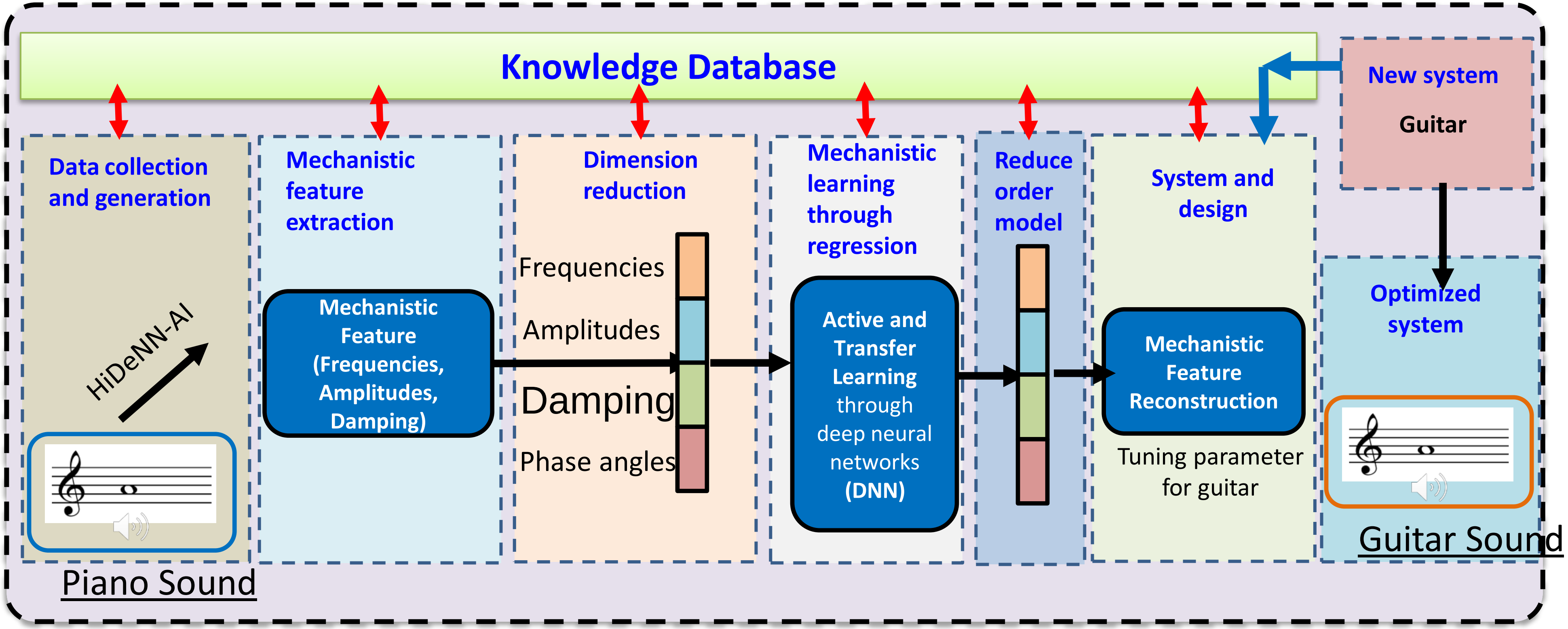

Data Collection and Generation (1)

- Start with training the **first** pair of A4 piano and A4 guitar sound files
- Sample rate: 44.1 kHz
- Duration: 2.8 second for the piano and 1.6 seconds for the guitar
- Then, repeat for the other **7 pairs of keys**: A5, B5, C5, C6, D5, E5, G5 piano and guitar sound files with duration ranging from 1.5 to 3.0 seconds. These **8** pairs of keys constitute the training sets.
- To reduce the data dimensions, the extracted four features using Short-time Fourier transform (STFT) and least square optimization for each data set is used for regression between the piano keys and the guitar keys (8x4x8 input, 8x4x8 output).

Data Collection and Generation (2)

A4 Dimension: $120{,}000\ (44.1\ kHz \times 2.8\ s)$

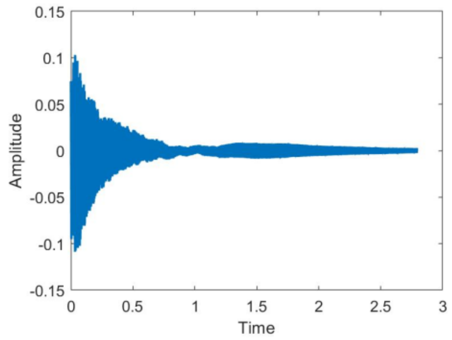

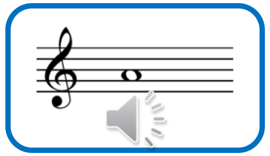

Piano Sound (A4)

A4 Dimension: $72{,}000\ (44.1\ kHz \times 1.6\ s)$

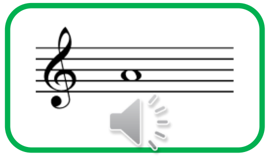

Guitar Sound (A4)

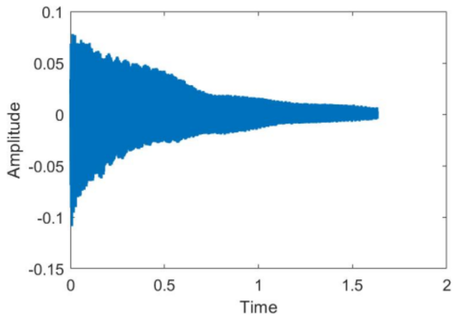

Piano [1]

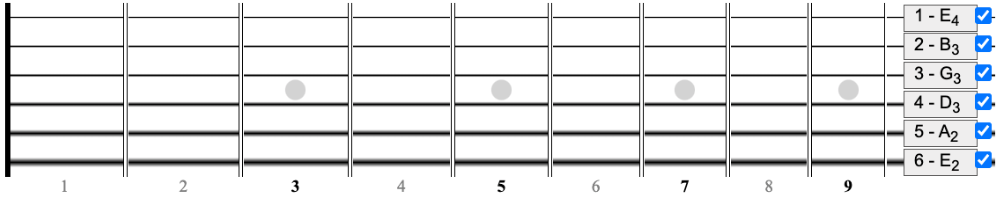

Guitar [1]

[1] https://www.apronus.com/

Mechanistic Feature Extraction

- To enhance the reconstruction of the authentic A4 key, Short Time Fourier Transform (STFT) is used to reveal the strike, sustain and decay.
  - **Definition:** The Short-time Fourier transform (STFT), is a Fourier-related transform used to determine the sinusoidal frequency and phase content of local sections of a signal as it changes over time.

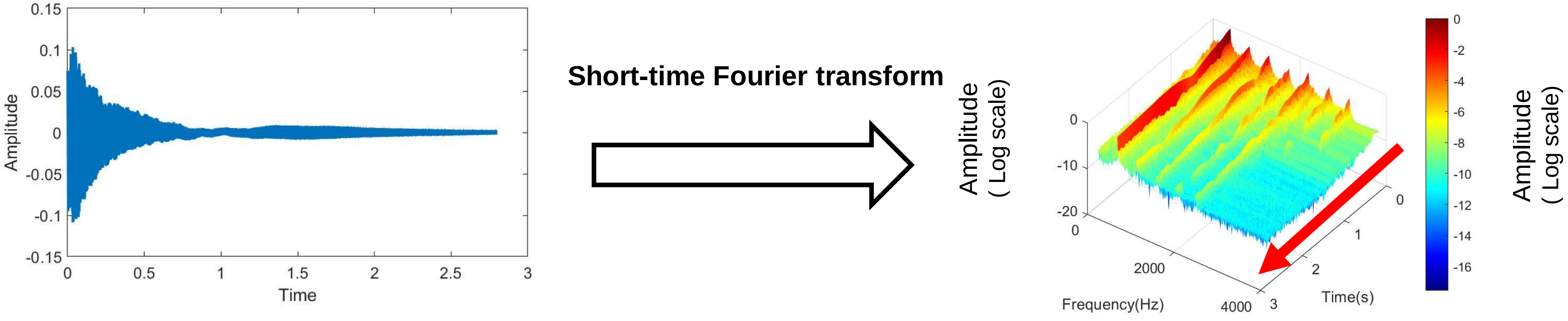

Signal

strike, sustain and decay

Dimension Reduction: Frequencies and Amplitudes

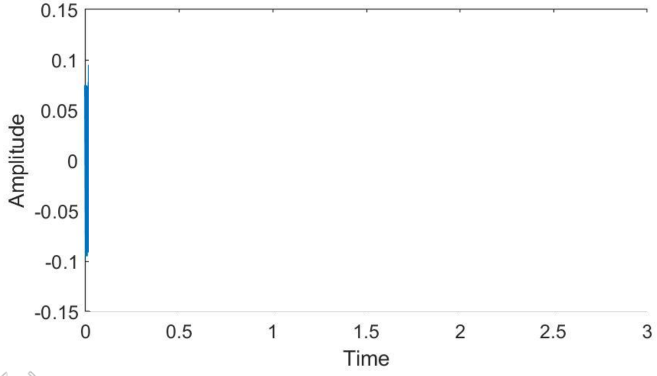

Authentic A4 piano sound

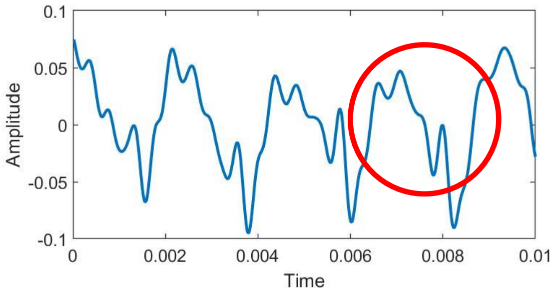

Zoom-in of the first 0.01 second depicts higher harmonics

0 to 0.01 second authentic A4 piano sound

STFT reveals higher frequencies sound signals disappear faster due to higher damping

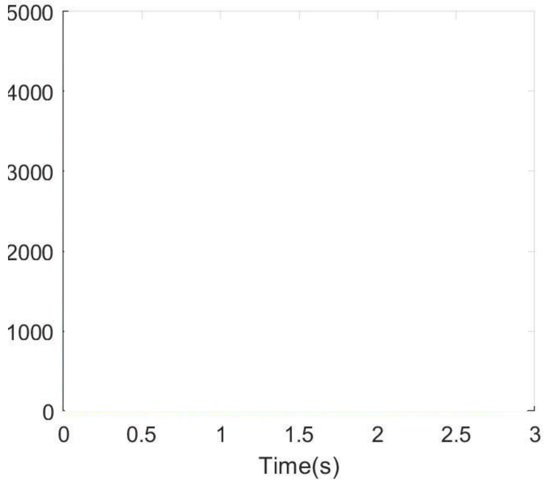

STFT: “authentic A4 piano” (2D view)

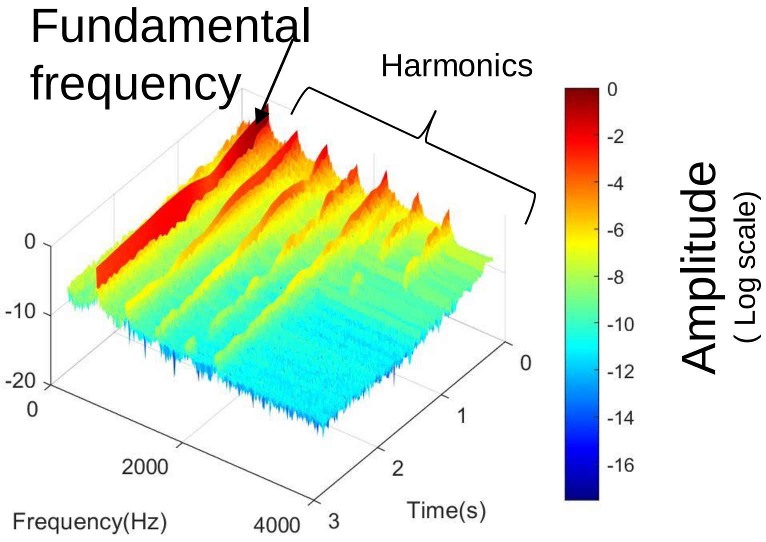

STFT of “authentic A4” (3D view)

Dimension Reduction: Damping Coefficients

- By using exponential fitting of time history, the values of each damping constant can be determined.
- The fitting can also be determined during the optimization stage using least square optimization.

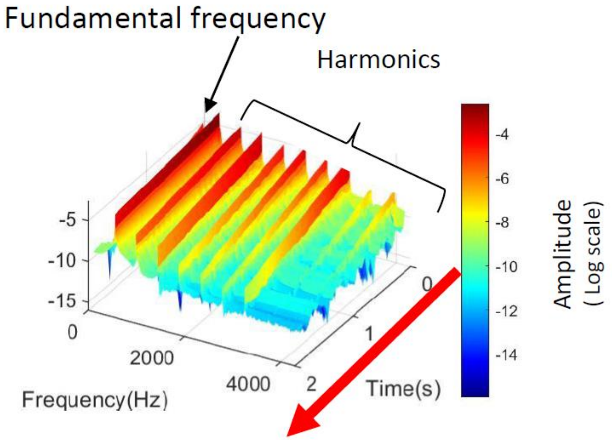

Mechanistic model

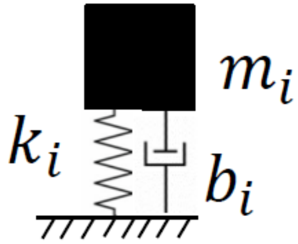

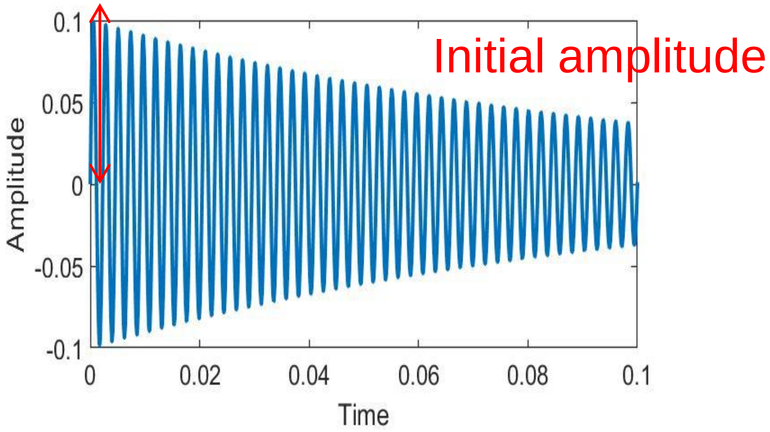

Damping of fundamental frequency i=1

$$y = \sum_{i=1}^{8} a_i e^{-b_i t} \sin(\omega_i t + \phi_i)$$

$$\begin{cases} a_i : \text{ initial amplitude} \\ b_i : \text{ damping ratio} \\ \omega_i : \text{ frequency} \\ \phi_i : \text{ phase angle} \end{cases}$$

Number of sampling points (features) in a sound file:

$$N_s = t \times fs = 842{,}310 \ \ (A4\ sound)$$

t: duration of the sound

fs: sampling rate

Features	$a_{i=1}$	$\omega_{i=1}$	$b_{i=1}$	$\phi_{i=1}$	...
Values	...	...	...	...	...

The number of features extracted is $4 \times 8 = 32$

Extracted Features of A4 Piano Sound and Guitar

All eight sets of features from authentic A4 piano and authentic A4 guitar sound

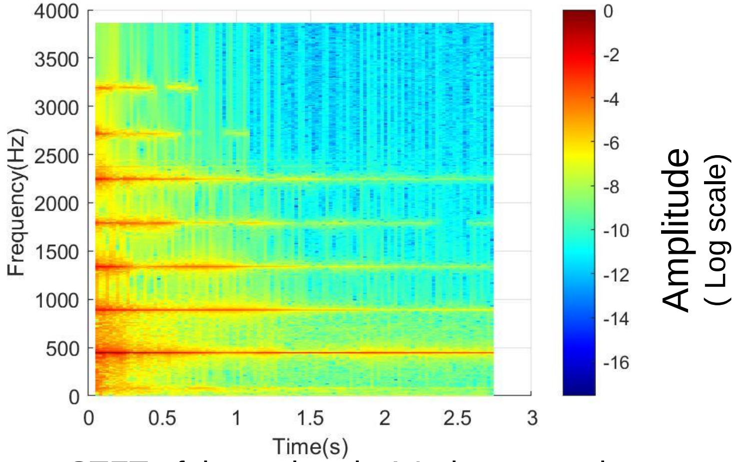

STFT of the authentic A4 piano sound

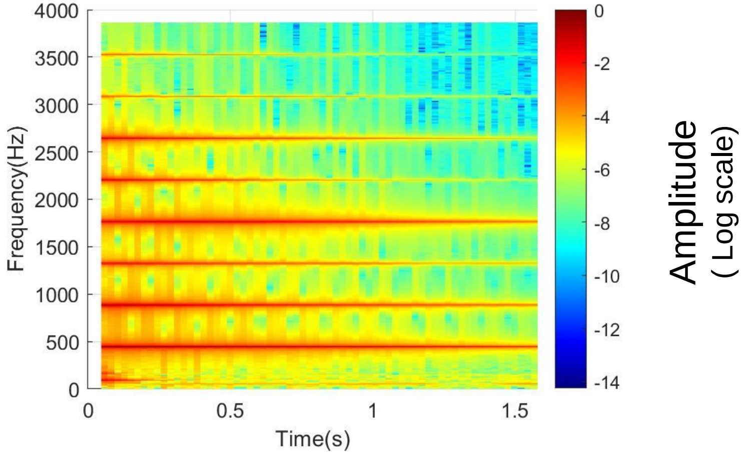

STFT of the authentic A4 guitar sound

Type	Frequencies (Hz)	Initial amplitudes	Damping coefficients	Phase angles (rad)
Fundamental	4.410E+02	1.034E-01	3.309E+00	6.954E-01
Harmonics	8.820E+02	1.119E-02	1.844E+00	7.202E-01
	1.323E+03	6.285E-03	5.052E+00	3.469E-01
	1.764E+03	7.715E-04	2.484E+00	5.170E-01
	2.205E+03	1.455E-03	8.602E+00	5.567E-01
	2.646E+03	5.130E-04	1.198E+01	1.565E-01
	3.087E+03	1.899E-04	8.108E+00	5.621E-01
	3.528E+03	3.891E-05	3.282E+00	6.948E-01

Optimal coefficients to reconstruct the authentic A4 piano sound

Type	Frequencies (Hz)	Initial amplitudes	Damping coefficients	Phase angles (rad)
Fundamental	4.400E+02	2.346E-02	1.287E+00	4.218E-01
Harmonics	8.800E+02	1.142E-02	1.865E+00	9.157E-01
	1.320E+03	3.630E-03	2.176E+00	7.922E-01
	1.760E+03	7.761E-03	1.100E+00	9.595E-01
	2.200E+03	7.860E-03	3.346E+00	6.557E-01
	2.640E+03	9.594E-03	2.504E+00	3.571E-02
	3.080E+03	1.088E-03	1.666E+00	8.491E-01
	3.520E+03	1.387E-03	2.610E+00	9.340E-01

Optimal coefficients to reconstruct the authentic A4 guitar sound

Dimension Reduction

Instrument	Original signal dimension	Reduced order dimension
Piano	120,000 (44.1 kHz $\times$ 2.8 s)	32 (4 features $\times$ 8 frequencies)
Guitar	72,000 (44.1 kHz $\times$ 1.6 s)	32 (4 features $\times$ 8 frequencies)

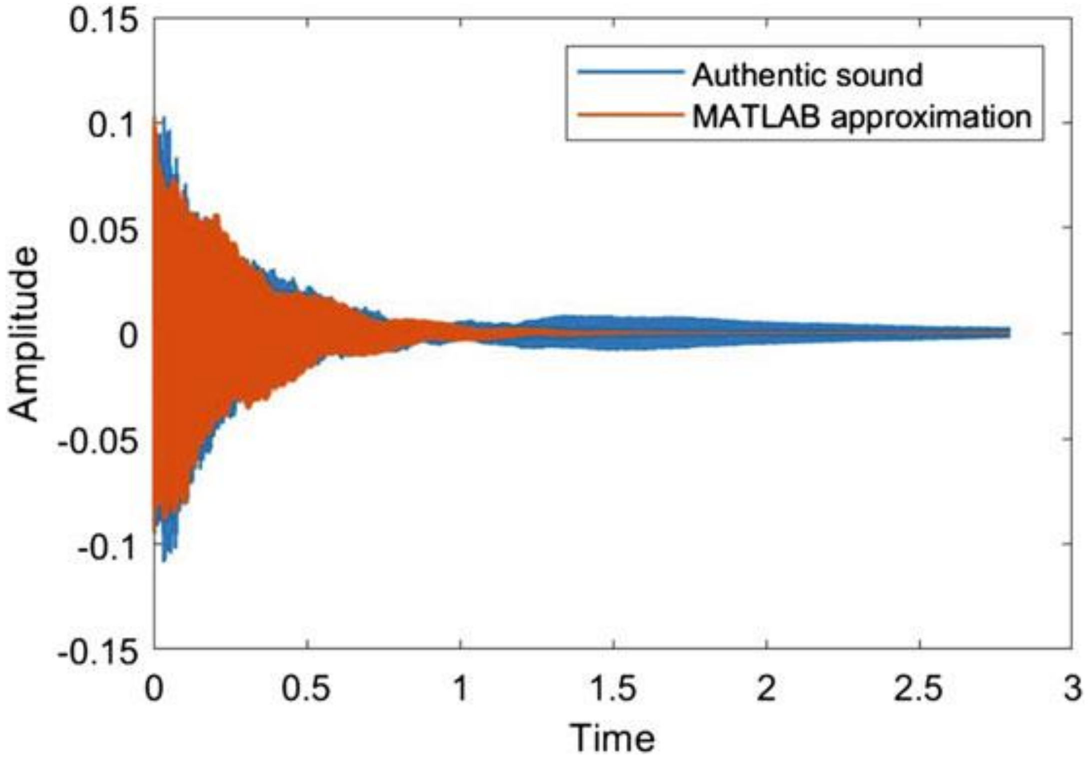

possibly due to reverberation or changing in the pressure from the damping pedal

Mechanistic Learning through Regression

Extracted Mechanistic features:
- 8 frequencies
- 8 amplitudes;
- 8 damping coefficient;
- 8 Phase angles;

Neural network:
- 3 hidden layers with 100 neurons;

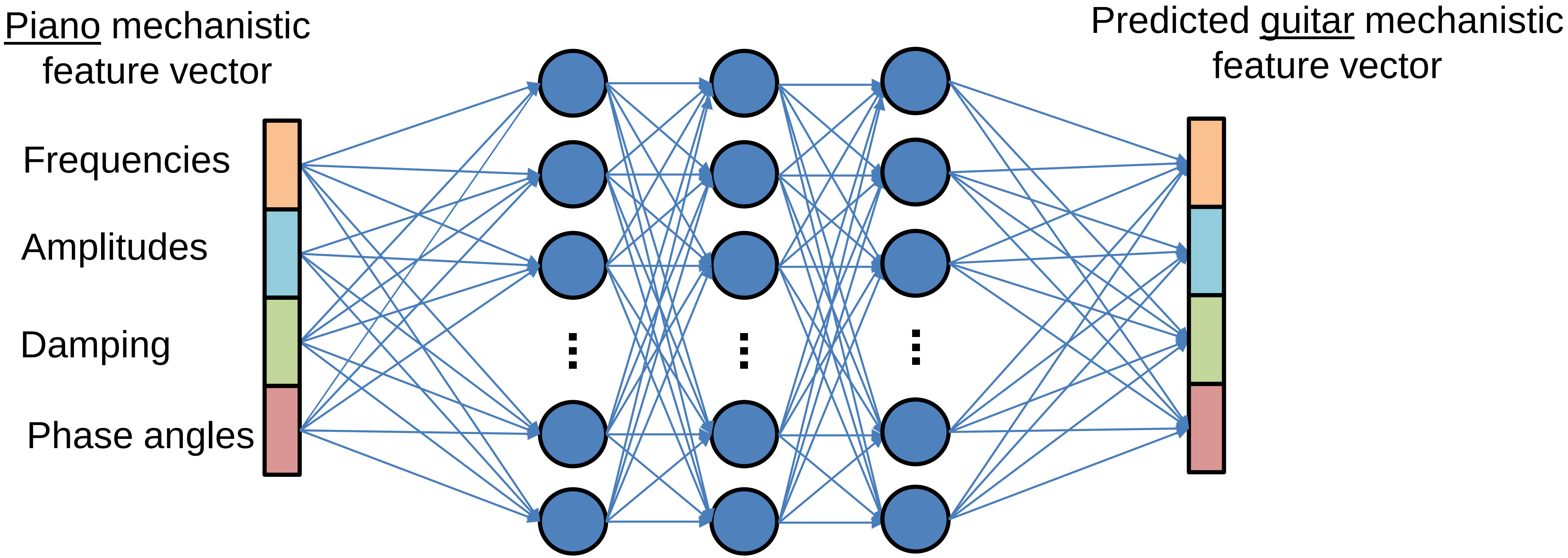

Generation of guitar sound is possible with a significantly smaller dimensions

Simple Demonstration of MDS for knowledge transfer in sound files

Learn from a system (Piano sound) and transfer the knowledge for a new system (Guitar sound)

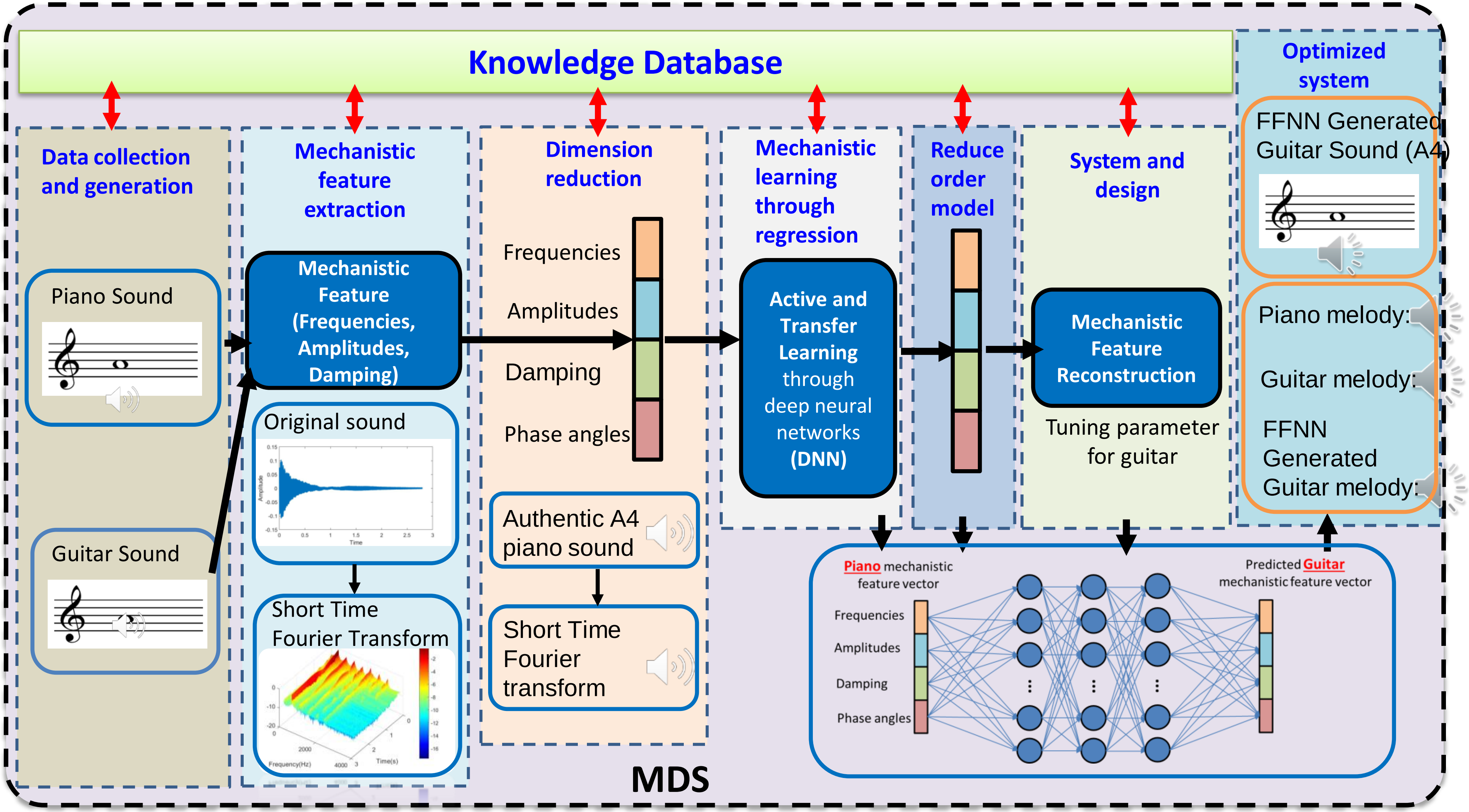

First seven notes from “Twinkle, twinkle little star”

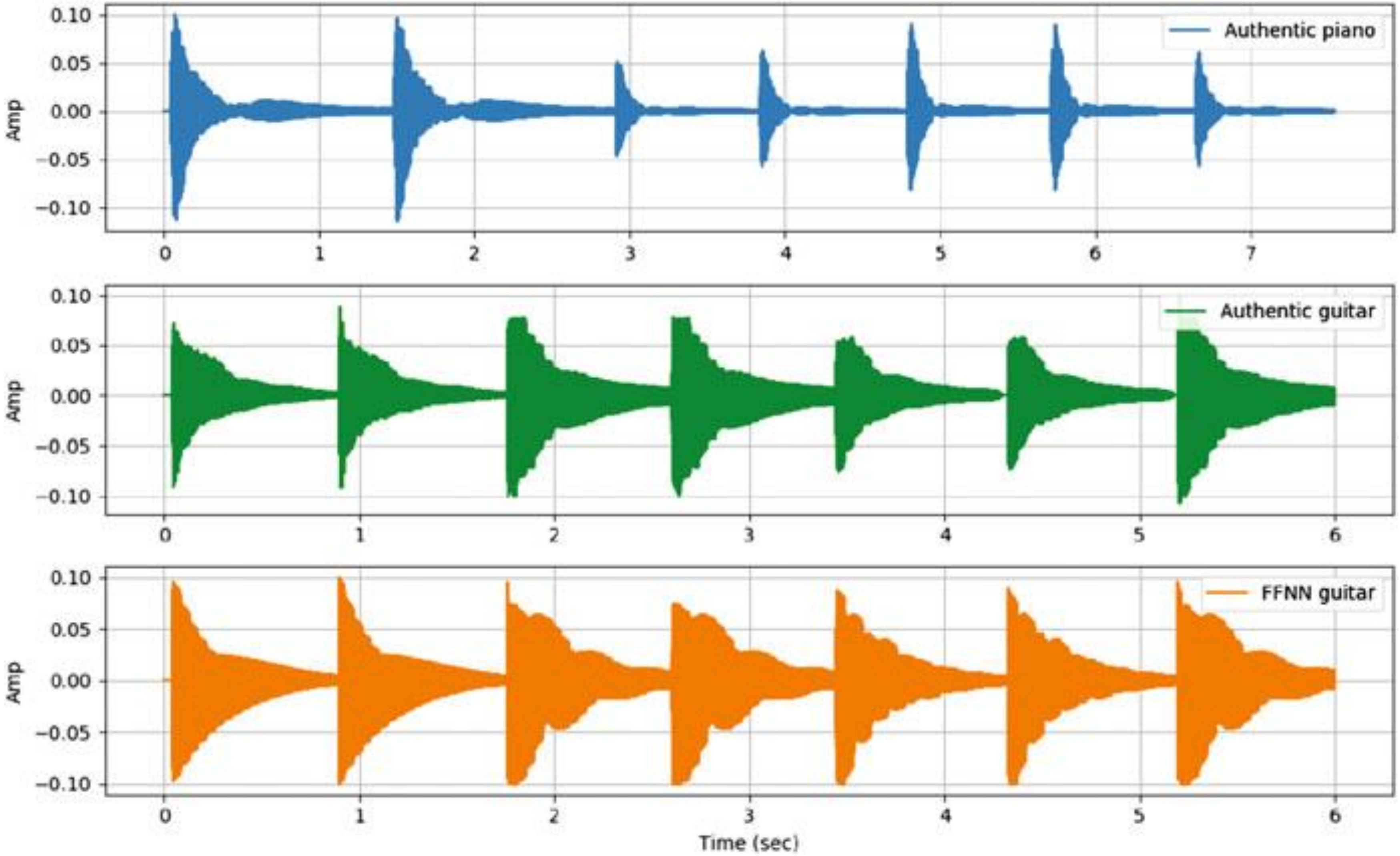

Musical Instrument Sound Conversion: Code

- Feature_extractor.m
- Sound_generator.m
- Model_trainer.py
- Feature_generator.py

Principal Component Analysis for Musical Note Conversion (Type 1 Advanced)

- Dimension reduction of the raw sound signals
- PCA creates a reduced order model based only on the data and does not consider mechanistic features → very hard to interpret
- Data Preprocessing (Normalization and Scaling)

$$
\begin{cases}
\text{piano sound signal:} \quad \underbrace{\mathbf{A}_p(m \times n)}_{\substack{m=8 \\ n=44{,}100\,Hz \times 1.86\,s \approx 81{,}849}} \xrightarrow[std(\mathbf{A}_p)]{mean(\mathbf{A}_p)} \mathbf{B}_p : \text{ normalized and scaled} \\
\text{guitar sound signal: } \mathbf{A}_g \xrightarrow[std(\mathbf{A}_g)]{mean(\mathbf{A}_g)} \mathbf{B}_g
\end{cases}
$$

Ap → Bp

$$
\text{Different keys } (m \text{ keys}) \quad
\begin{array}{c}
A4 \\ A5 \\ B5 \\ \vdots \\ E5
\end{array}
\begin{bmatrix}
\boxed{1483 \; 1369 \; 1285 \; \cdots \; 332} \\
1590 \; 1565 \; 1446 \; \cdots \; 109 \\
715 \;\; 577 \;\; 436 \; \cdots \; 234 \\
\vdots \qquad \ddots \qquad \vdots \\
2901 \; 3091 \; 3214 \; \cdots \; 32
\end{bmatrix}
$$

Time (n time steps)

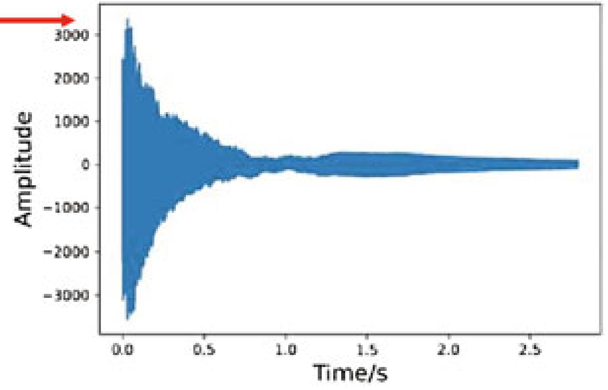

Signal for A4 key in piano

$$
\text{Different keys } (m \text{ keys}) \quad
\begin{array}{c}
A4 \\ A5 \\ B5 \\ \vdots \\ E5
\end{array}
\begin{bmatrix}
\frac{1483 - 184.00}{1455.67} & \frac{1369 - 185.75}{1368.17} & \frac{1285 - 171.25}{1255.69} & \cdots & \frac{32 - 16.37}{15.32} \\
\frac{1590 - 184.00}{1455.67} & \frac{1565 - 185.75}{1368.17} & \frac{1446 - 171.25}{1255.69} & \cdots & \frac{19 - 16.37}{15.32} \\
\frac{715 - 184.00}{1455.67} & \frac{577 - 185.75}{1368.17} & \frac{436 - 171.25}{1255.69} & \cdots & \frac{24 - 16.37}{15.32} \\
\vdots & \vdots & & \ddots & \vdots \\
\frac{2901 - 184.00}{1455.67} & \frac{3091 - 185.75}{1368.17} & \frac{3214 - 171.25}{1255.69} & \cdots & \frac{12 - 16.37}{15.32}
\end{bmatrix}
$$

Time (n time steps)

Principal Component Analysis for Musical Note Conversion (Type 1 Advanced)

- Compute the Eigenvalues and Eigenvectors for the Covariance Matrix of Bp and Bg
- Build a Reduced-Order Model

$$\text{covariance: } \mathbf{X}_p = \frac{\mathbf{B}_p{}^T\mathbf{B}_p}{n-1} = \mathbf{P}_p\mathbf{\Lambda}\mathbf{P}_p{}^T = \begin{bmatrix}\mathbf{p}_1 & \mathbf{p}_2 & \cdots & \mathbf{p}_m\end{bmatrix}\begin{bmatrix}\lambda_1 & 0 & \cdots & 0\\ 0 & \lambda_2 & \cdots & 0\\ \vdots & \vdots & \ddots & \vdots\\ 0 & 0 & \cdots & \lambda_m\end{bmatrix}\begin{bmatrix}\mathbf{p}_1{}^T\\ \mathbf{p}_2{}^T\\ \vdots\\ \mathbf{p}_m{}^T\end{bmatrix}$$

$$\begin{cases}\mathbf{P}_p: \text{ orthogonal matrix containing the eigenvectors}\\ \mathbf{\Lambda}: \text{ diagonal matrix containing the eigenvalues}\end{cases}$$

$$\rightarrow \text{reduced-order model: } \underbrace{\mathbf{R}_p}_{(m\times m)} = \underbrace{\mathbf{B}_p}_{(m\times n)}\underbrace{\mathbf{P}_p}_{(n\times m)} = \begin{bmatrix}\mathbf{a}_1{}^T\\ \mathbf{a}_2{}^T\\ \vdots\\ \mathbf{a}_m{}^T\end{bmatrix}$$

Magnitude for each PC	Piano-A4	Guitar-A4
1st PC	−78.08	−47.32
2nd PC	303.93	−3.18
3rd PC	47.98	19.68
4th PC	−5.03	27.26
5th PC	−38.21	−40.95
6th PC	−5.68	19.26
7th PC	−4.71	144.83
8th PC	1.45×10^{-13}	3.58×10^{-14}

$\mathbf{a}_i\,(m\times 1)$ contains the magnitudes of all principal components (PCs) for the i-th piano sound

Principal Component Analysis for Musical Note Conversion (Type 1 Advanced)

- Inverse Transform Magnitudes for all PCs to a Sound
- Cumulative Energy for Each PC

$$\rightarrow \text{reduced-order model: } \underset{(m\times m)}{\mathbf{R}_g} = \underset{(m\times n)}{\mathbf{B}_g} \underset{(n\times m)}{\mathbf{P}_g} = \begin{bmatrix} \mathbf{b}_1{}^T \\ \mathbf{b}_2{}^T \\ \vdots \\ \mathbf{b}_m{}^T \end{bmatrix}$$

$\mathbf{b}_i\left(m\times 1\right)$ contains the magnitudes of all principal components (PCs) for the i-th guitar sound

$$\rightarrow \text{reconstruct guitar sound: } \mathbf{s}_i = \mathbf{b}_i{}^T \mathbf{P}_g{}^T \circ std\left(\mathbf{A}_g\right) + mean\left(\mathbf{A}_g\right)$$

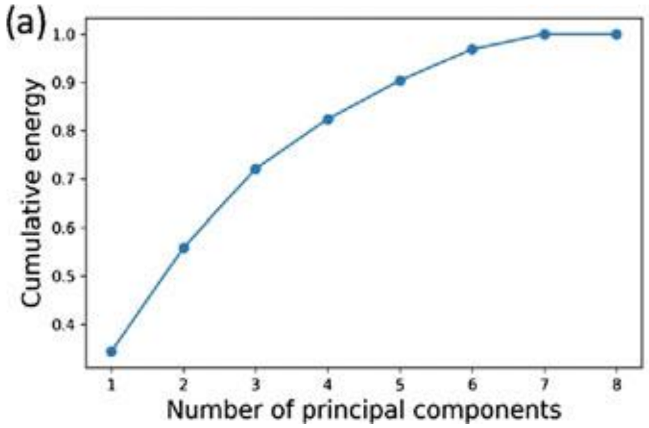

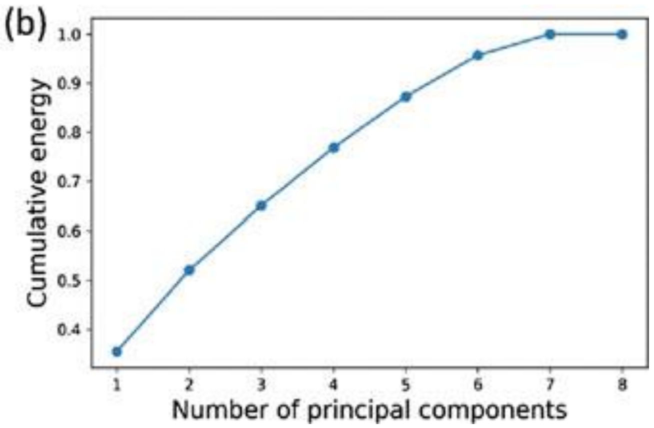

$$e_i = \frac{\sum_{k=1}^{i}\left(\lambda_k\right)^2}{\sum_{k=1}^{m}\left(\lambda_k\right)^2}$$

Principal Component Analysis for Musical Note Conversion (Type 1 Advanced)

- Training a Fully-Connected FFNN

$$\left(\mathbf{a}_i,\ i=1,\ldots,8\right)\rightarrow \mathbb{F}_{\text{FFNN}}\rightarrow\left(\mathbf{b}_i,\ i=1,\ldots,8\right)$$

$$\begin{cases}\text{training}:\ L=\dfrac{1}{N}\displaystyle\sum_{i=1}^{N}\left(\mathbf{b}_i-\hat{\mathbf{b}}_i\right)^2\\ \text{prediction:}\ \hat{\mathbf{b}}_i=\mathbb{F}_{\text{FFNN}}\left(\mathbf{a}_i\right)\end{cases}$$

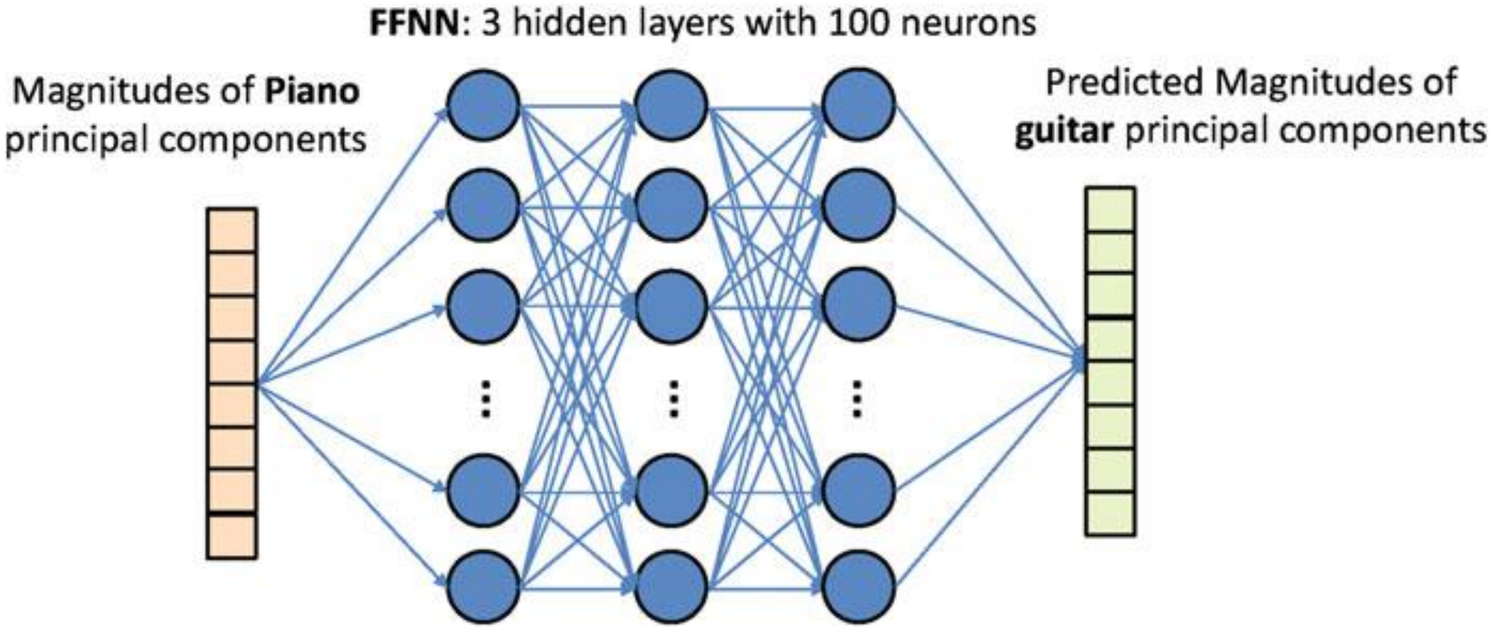

Principal Component Analysis for Musical Note Conversion (Type 1 Advanced)

- Generate a Single Guitar

$$\text{well-trained FFNN model is obtained} \rightarrow \hat{\mathbf{b}} = \mathbb{F}_{\text{FFNN}}\left(\mathbf{a}\right)$$

$$\rightarrow \text{reconstruct the guitar sound: } \hat{\mathbf{s}}_g = \hat{\mathbf{b}}^T \mathbf{P}_g{}^T \circ std\left(\mathbf{A}_g\right) + mean\left(\mathbf{A}_g\right)$$

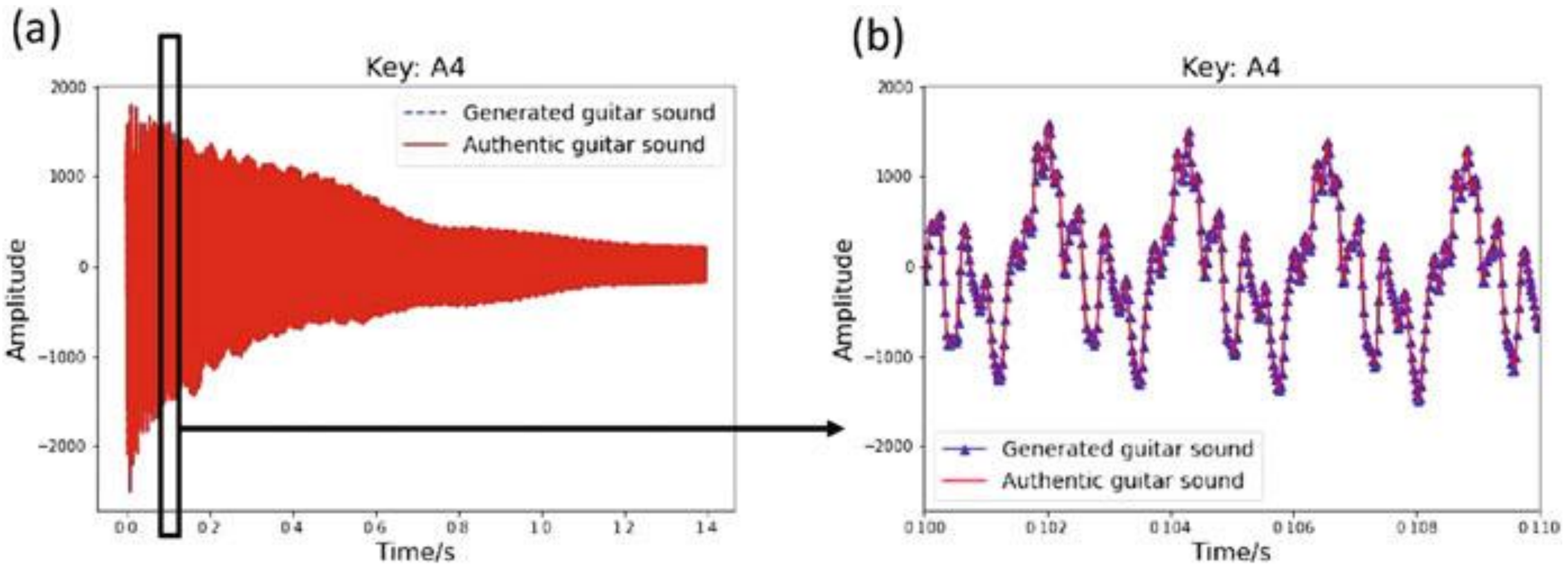

Principal Component Analysis for Musical Note Conversion (Type 1 Advanced): Code

- Python code for data collection and data preprocessing
- PyTorch is used to implement the FFNN and to train the model
- Inverse transform Python code
- The generation of a melody: “Twinkle, twinkle little star”
  - “C5, C5, G5, G5, A5, A5, G5”

npj Computational Materials

www.nature.com/npjcompumats

ARTICLE OPEN

Check for updates

Mechanistic data-driven prediction of as-built mechanical properties in metal additive manufacturing

Xiaoyu Xie[1,4], Jennifer Bennett[1,2,4], Sourav Saha[3,4], Ye Lu[1], Jian Cao[1], Wing Kam Liu[1]✉ and Zhengtao Gan[1]✉

Metal additive manufacturing provides remarkable flexibility in geometry and component design, but localized heating/cooling heterogeneity leads to spatial variations of as-built mechanical properties, significantly complicating the materials design process. To this end, we develop a mechanistic data-driven framework integrating wavelet transforms and convolutional neural networks to predict location-dependent mechanical properties over fabricated parts based on process-induced temperature sequences, i.e., thermal histories. The framework enables multiresolution analysis and importance analysis to reveal dominant mechanistic features underlying the additive manufacturing process, such as critical temperature ranges and fundamental thermal frequencies. We systematically compare the developed approach with other machine learning methods. The results demonstrate that the developed approach achieves reasonably good predictive capability using a small amount of noisy experimental data. It provides a concrete foundation for a revolutionary methodology that predicts spatial and temporal evolution of mechanical properties leveraging domain-specific knowledge and cutting-edge machine and deep learning technologies.

npj Computational Materials (2021)7:86 ; https://doi.org/10.1038/s41524-021-00555-z

Metal Additive Manufacturing is the Buzzword Nowadays

https://phys.org/news/2017-12-additive.html

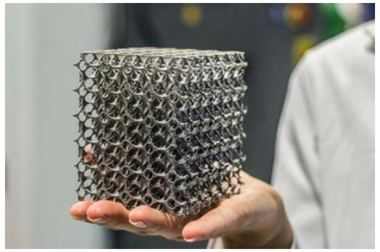

Complex parts

Metal Additive Manufacturing

Hip implant

Courtesy GE)

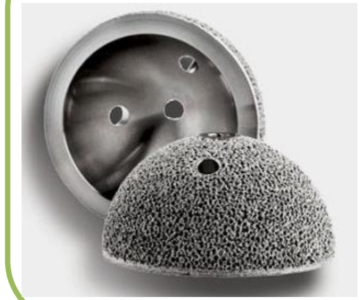

Courtesy Siemens

Turbine blades

https://www.youtube.com/watch?v=bQMWETpckNU

https://www.globenewswire.com/news-release/2019/06/05/1864873/0/en/SmarTech-Analysis-Issues-Latest-Report-on-Metal-Additive-Manufacturing-Market.html

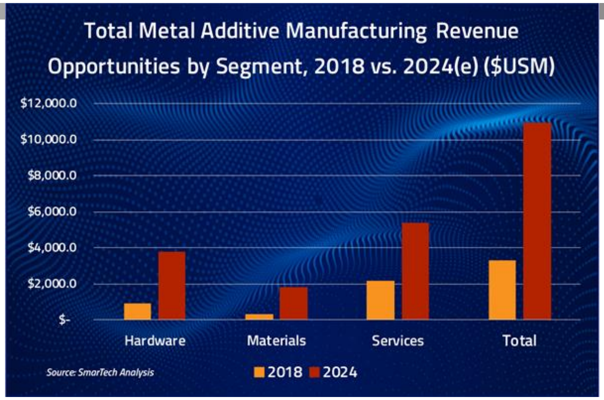

Revenue Opportunities

Perez, K. Blake. "Design Innovation with Additive Manufacturing (AM): An AM-Centric Design Innovation Process." *Singapore University of Technology and Design* (2018).

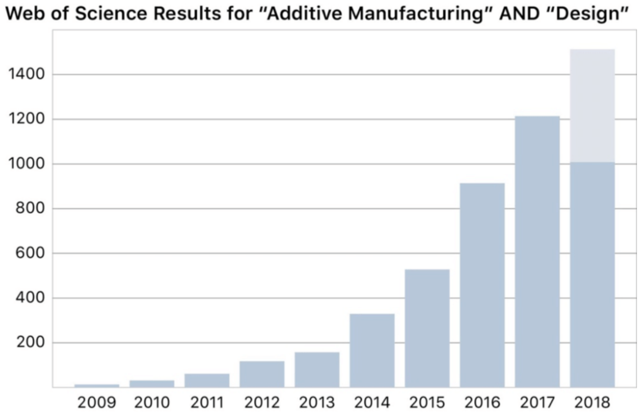

Number of papers with additive manufacturing and design in it

There are some structural defects in parts coming from the Process

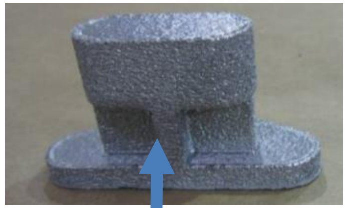
Surface Roughness

Porosity

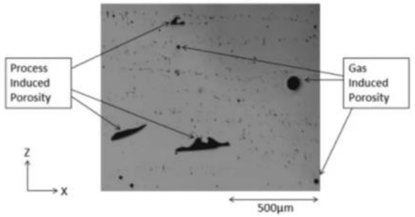

Defects

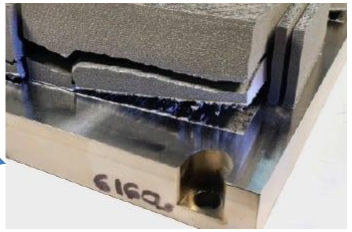
Residual stress


Delamination

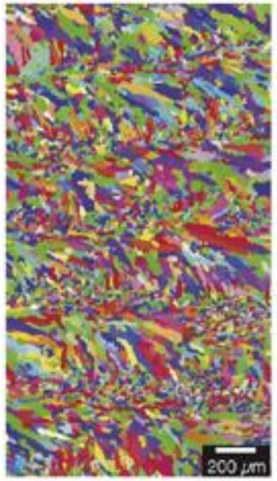

Microstructural Heterogeneity

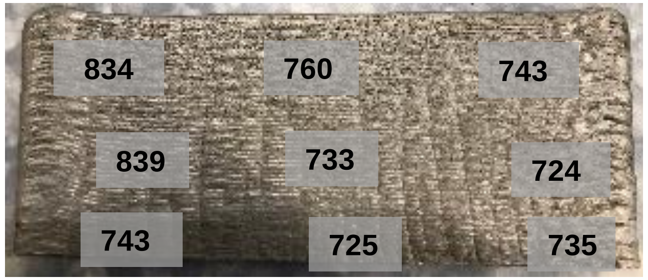

At different points we see different ultimate tensile strength

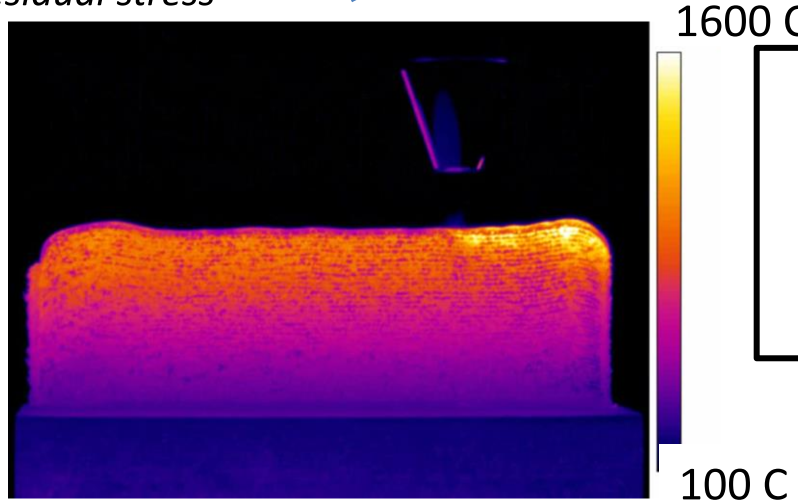

Source of all these defects is high thermal gradient and solidification rate!

Can we control and design the thermal history at each point and get AM part with desired property?

System and Design Philosophy

System Description:

- Metal additive manufacturing system (can be either Direct Energy Deposition (DED) or Powder bed) where we can control the manufacturing process parameters.
- We can measure the thermal response of the system with Infrared imaging system.
- We can only test the mechanical properties at a few locations on the wall with tensile test.

Modeling Objective:

Our objective is to develop a *computational* model that takes the thermal history at different points on the AM build wall and can predict the mechanical property (for example, ultimate tensile strength) at that point.

Design Objective:

- To design the AM process parameters (scan speed or laser power).
- To control the temperature history at different locations.
- To minimize the variation of mechanical properties at different locations of the build.

Modeling approach: Mechanistic data science and Digital Twins

Mechanistic Data Science and Digital Twins for System and Design

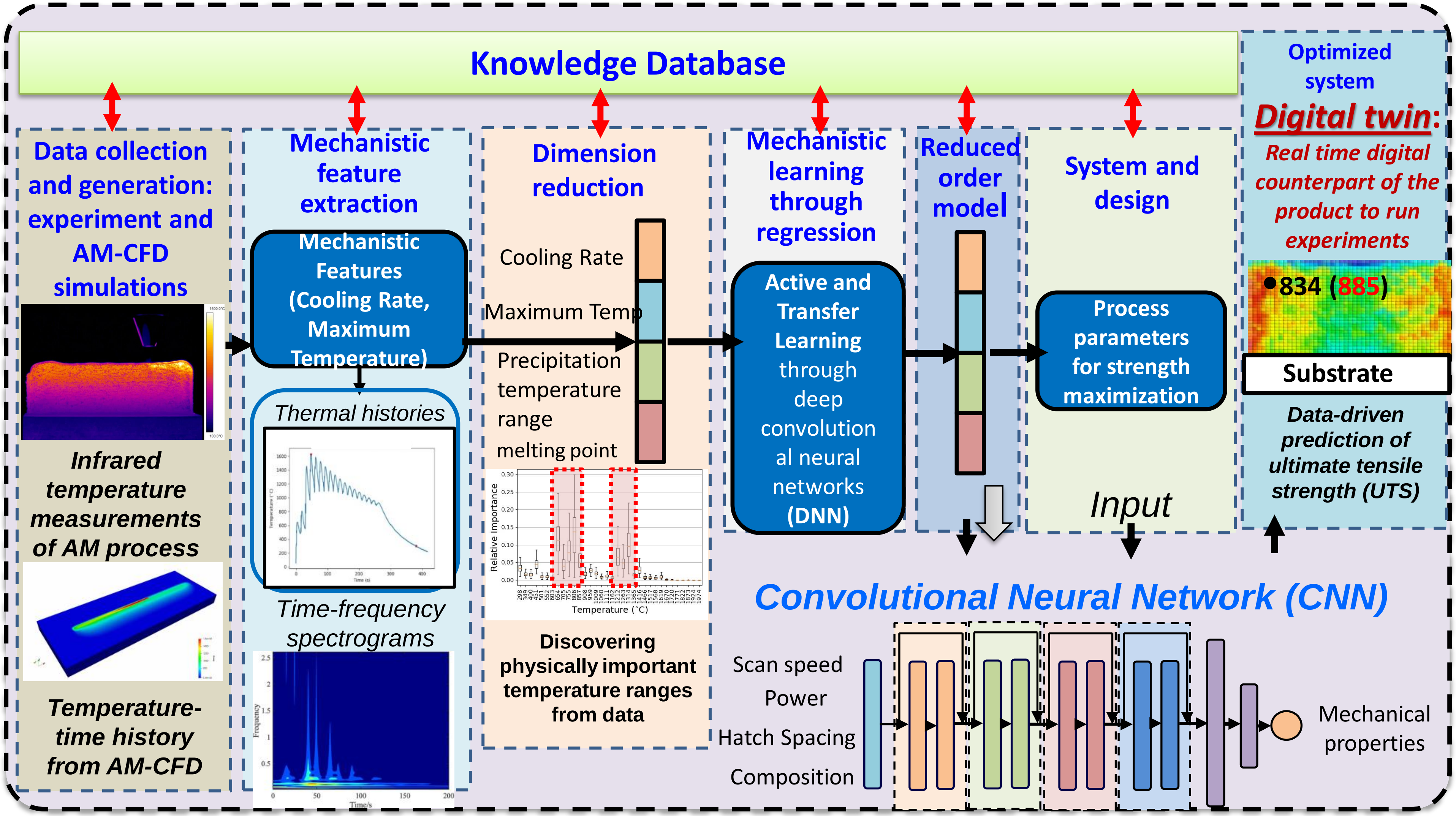

Some important Definition for Metal Additive Manufacturing

Liquidus Temperature: The temperature above which all components of the alloys are liquid.
Solidus Temperature: The temperature below which all components of the alloys are solid.
Solidification Cooling Time: The time required for the alloy to change from the liquid to solid phase during cooling.

Solidification Cooling Rate: The slope of the temperature-time history during solidification.

Dwell time: The pause between deposition between two successive layers.
Meltpool Control: Controlling the laser power to maintain a desired meltpool characteristics.

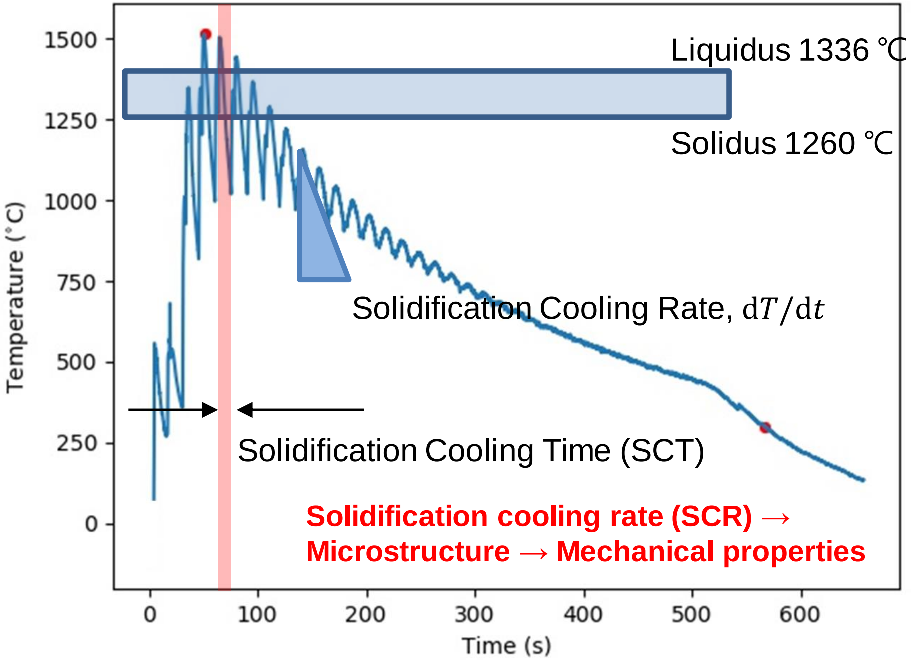

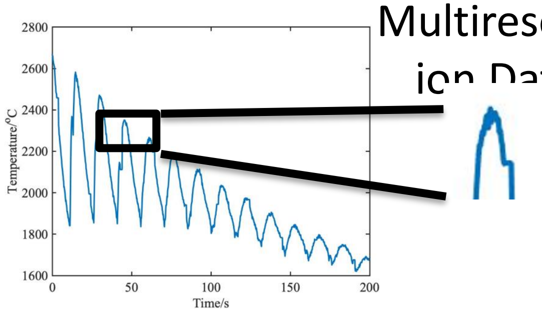

Multiresolut
ion Data

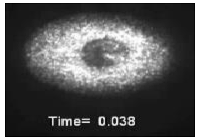

Meltpool dynamics (ns ~ ms)

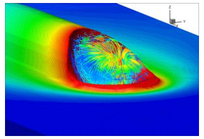

Convection and radiation cooling (s)

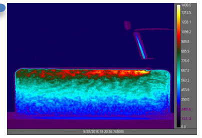

Scan speed (ms)

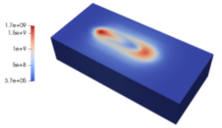

Residual plastic stress (s)

Sources of data from multiple time scales

Local Thermal History is the Key Factor Controlling Physical Phenomena

Multilayer AM Process

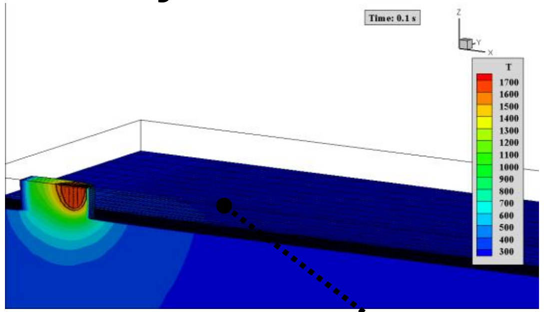

2. Vaporization/Spattering

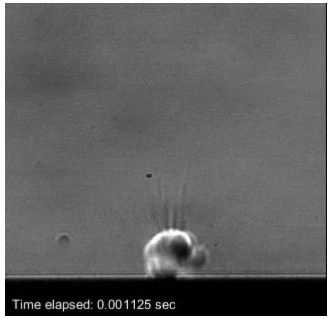

Loss of heat, mass and composition

Bidare, P., et al. 142 (2018): 107-120.

3. Solidification

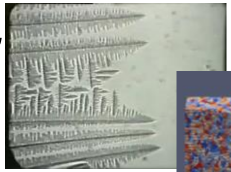

https://www.youtube.com/watch?v=S07fPo45BvM

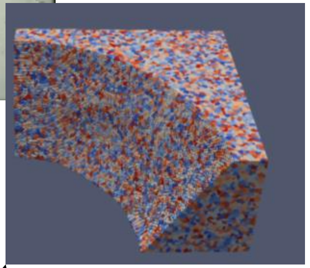

Grain growth
Dendrite
Segregation
Precipitate

1. Melt Pool Dynamics

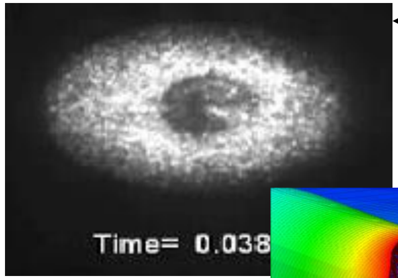

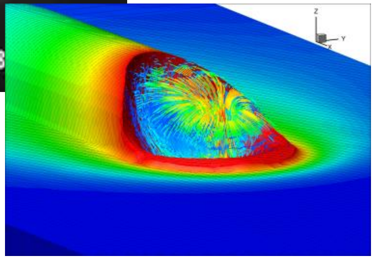

Heat absorption
Mass addition
Marangoni flow
Radiation

Zhao, C. X., et al. 58.19 (2010): 6345-6357.

4. Solid-State Phase Transformation

Grain growth
Precipitate
Phase change

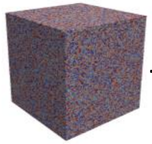

Microstructure depends on temperature gradient, growth velocity and cooling rate

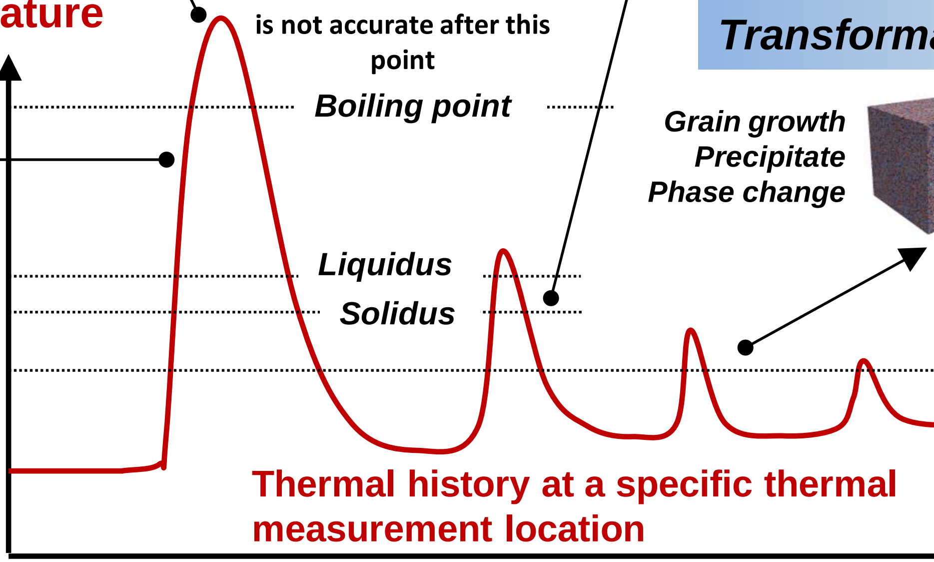

Assumption 1: thermal field includes enough information for explanation/prediction of mechanical properties of a specific alloy system.

Overview of the Process Features

Material System	IN 718; Substrate: SS 304
Manufacturing Method	Direct Energy Deposition
Machine	DMG-MORI LaserTech65
Particle Size	50 – 150 µm
Laser Power	1800 W
Powder Flow	18 g/min
Scanning Speed	1000 mm/min
Laser Spot	3 mm
Wall Length	Set 1: 80 mm (3 walls, No dwell time) Set 2: 120 mm (3 walls, No dwell time) Set 3: 120 mm (3 walls, 5s dwell time) Set 4: 120 mm (3 walls, melt pool control)

Input Process Features

1. No Dwell Time
2. 5 second Dwell Time
3. Meltpool Control

Mechanistic Signature

Temperature-time history

Mechanical Property

1. Ultimate tensile strength
2. Elongation
3. Yield strength
4. Young’s modulus

Position-dependent Mechanical Properties as the Output

Thermal histories at the center of ROIs in each wall (9-12 locations per wall)

Experimental IR sensing

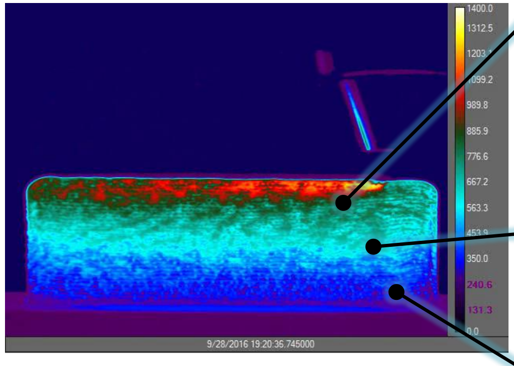

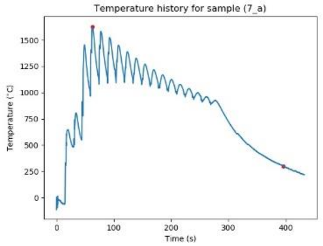

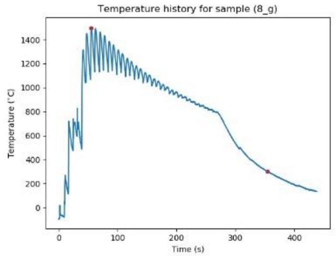

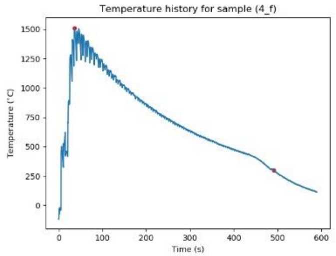

12 thin walls with different process conditions

Process conditions:

1. **Without Dwell**
2. **With 5s Dwell Time**
3. **Meltpool Control**

⋮

135 thermal curves

Input

Small tensile coupons at corresponding ROIs of the walls

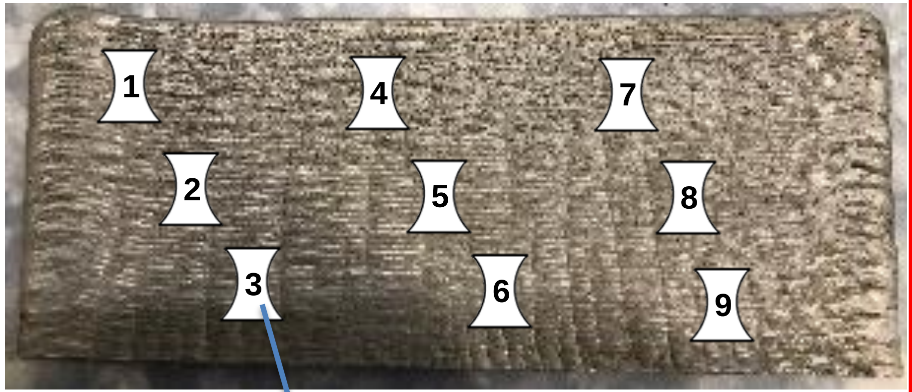

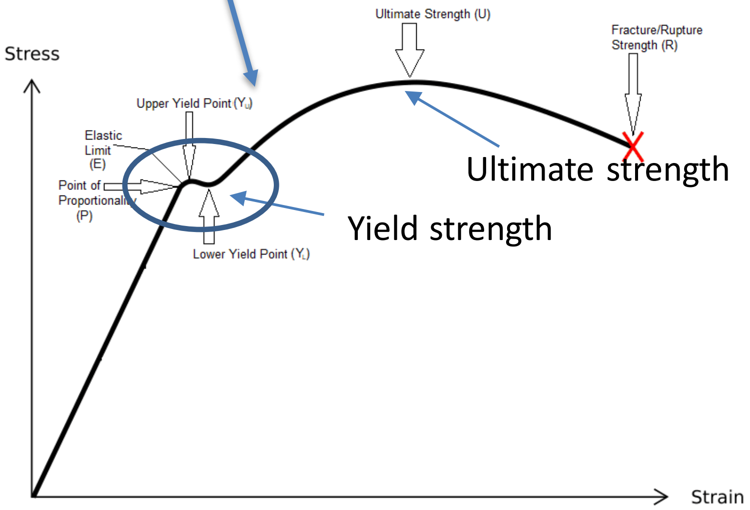

Stress-strain curve
135 sets of mechanical properties

Output

Wavelet scalograms encapsulates multiresolution Information

- **Morse wavelet [1]:** $\psi_{a,b}(\omega) = U(\omega) c_{a,b} \omega^{a} e^{-\omega b}$
- **Wavelet transform:** $W(a,b) = \int_{-\infty}^{\infty} f(t)\psi^{*}_{a,b}(t)\,dt$

Thermal history

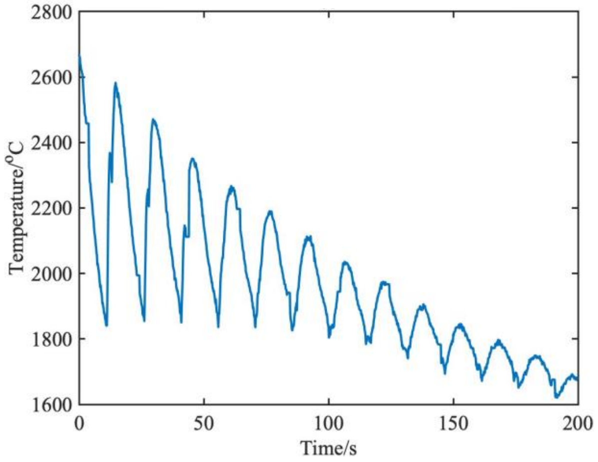

Wavelet scalogram

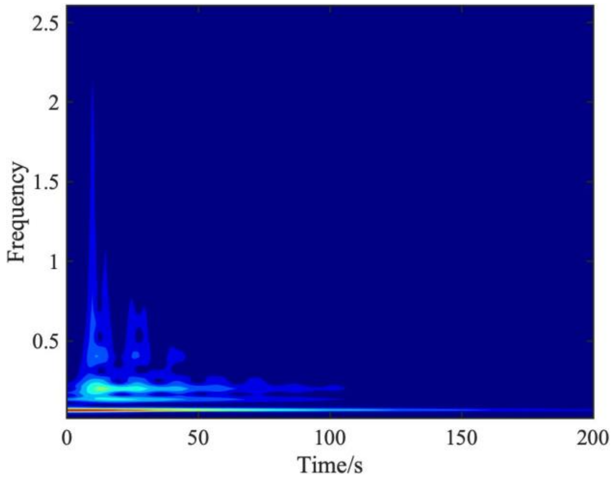

Wavelet scalogram with logarithmic y-axis

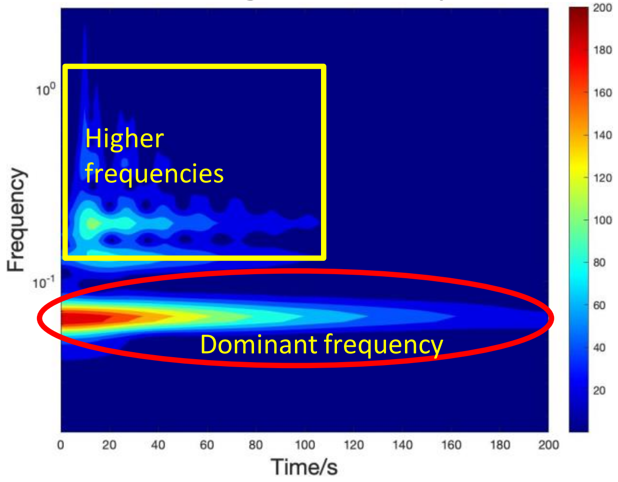

- Temperature-time plot is converted to Frequency-time plot using wavelet transform.
- Frequency axis is converted from decimal to logarithmic axis for readability.

- *Dominant frequency* of 0.1 Hz is related to *laser scan speed*.
- *High frequencies* are related to *meltpool shape change*, *instantaneous temperature fluctuation* and *inherent noise.*

[1] Olhede, S. C. et al. “Generalized morse wavelets.” IEEE Transactions on Signal Processing, 2002.

Thermal response is dependent on the location on the wall

- **location 1 (top):** *dual peaks appearance*---does not get enough time to cool before reheating.
- **Location 2 (bottom right):** *more fluctuation*---multiple layers are deposited, experiences more heating and cooling cycles, more complex frequency spectrum.

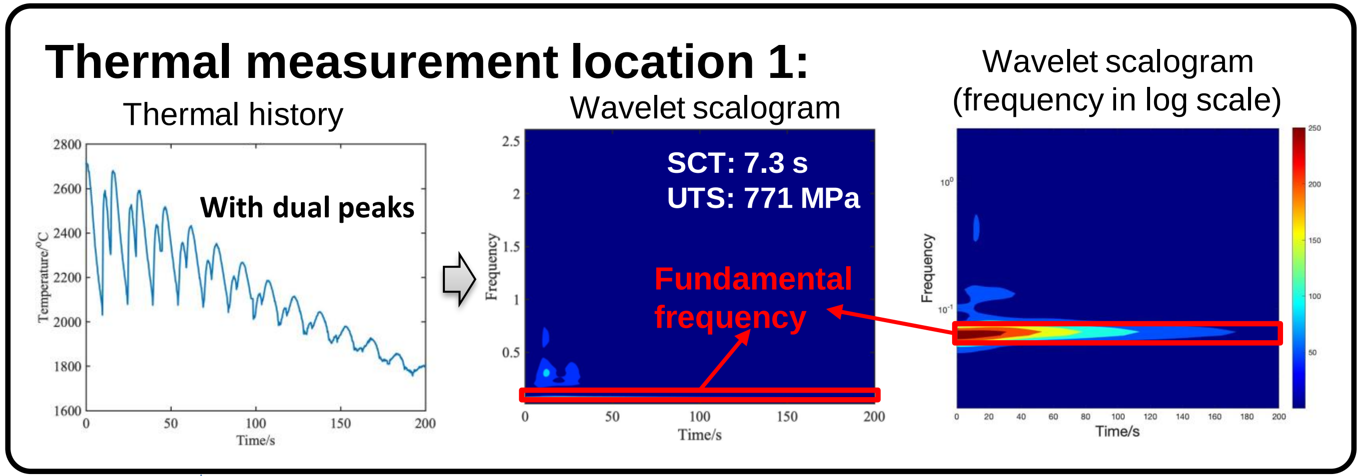

Location 2: higher solidification cooling rate resulting in *higher volume fraction and finer precipitates*, hence ***higher strength***.

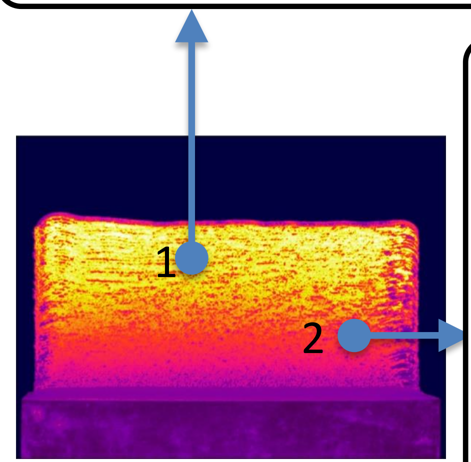

120 mm thin wall without dwell time

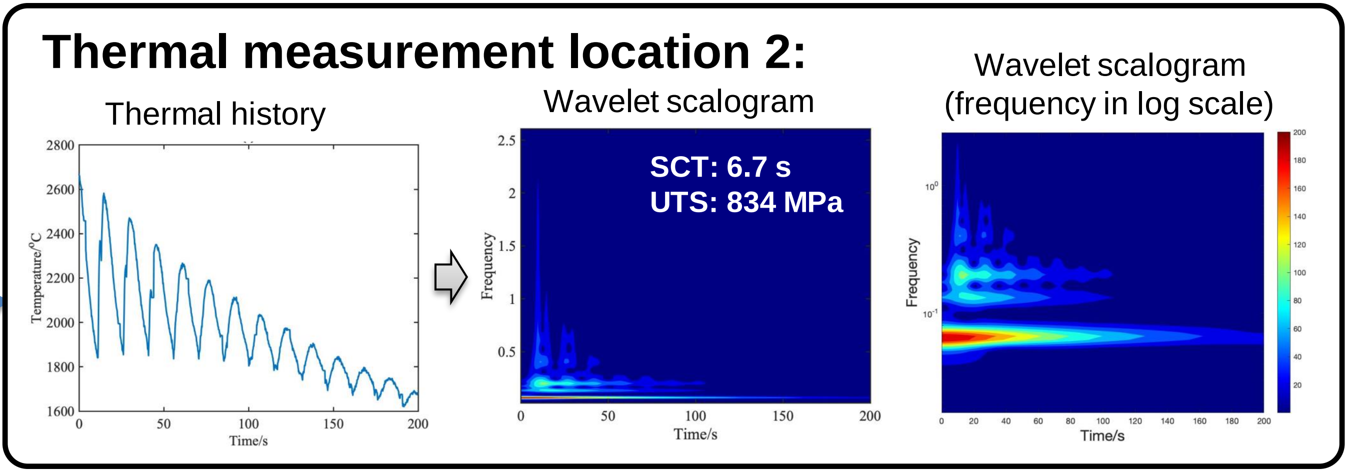

Dwell time introduces higher fluctuations in temperature

With dwell time: higher frequencies appear on the frequency-time spectrum; because it has more time to get cooled before reheated.

Without dwell time: solidification cooling time is lower, hence, more precipitates form (strengthening).

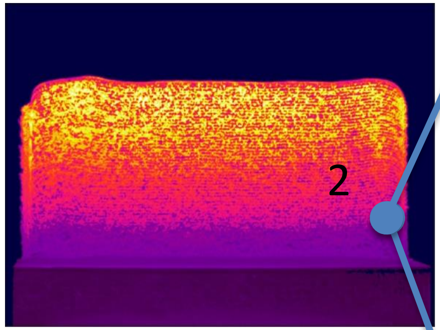

120 mm thin wall

Thermal measurement location 2:

Thermal history | Wavelet scalogram | Wavelet scalogram (frequency in log scale)

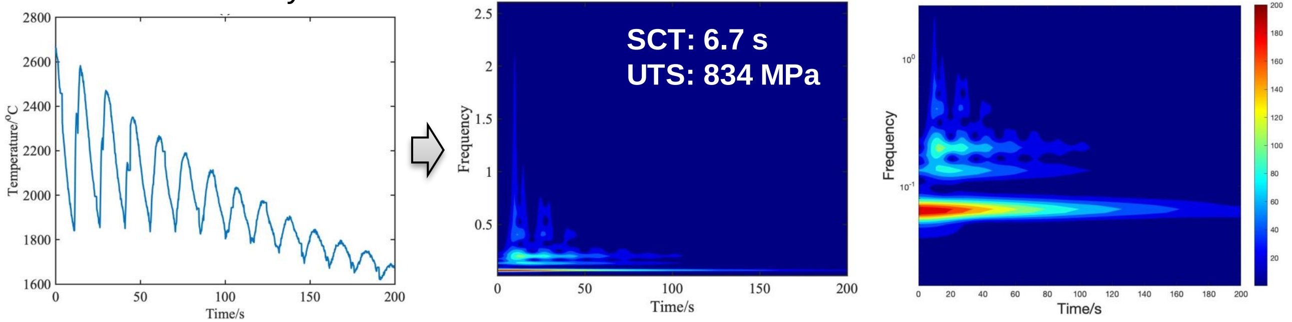

Without dwell time

Thermal measurement loca

Thermal history | Wavelet scalogram | Wavelet scalogram (frequency in log scale)

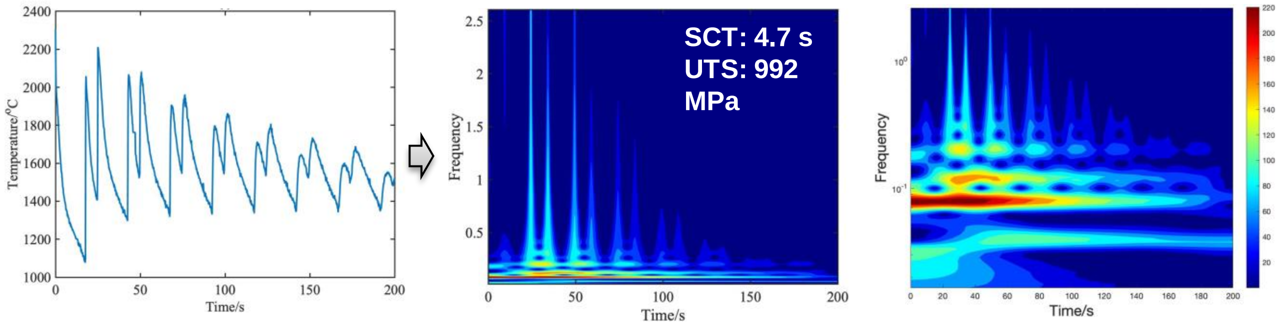

With 5 s dwell time

Meltpool control makes fluctuations more consistent

Melt pool control gives less thermal history fluctuation, shown in wavelet scalograms.

Thermal history | Magnification plot of a sub-range thermal history | Wavelet scalogram (frequency in log scale)

With melt pool control

Without melt pool control

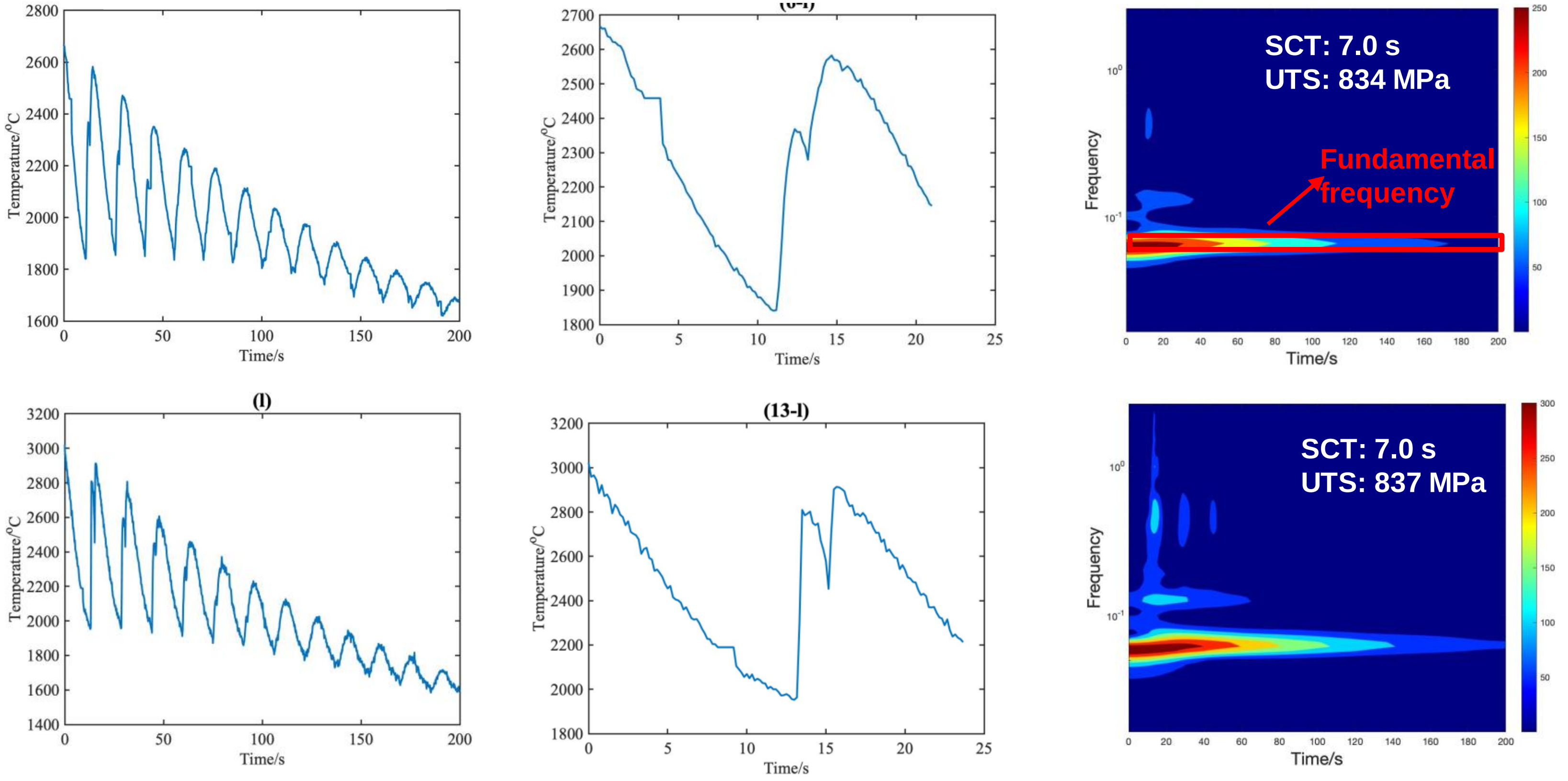

Discovery of Physics insight from Temperature: Binning Technique

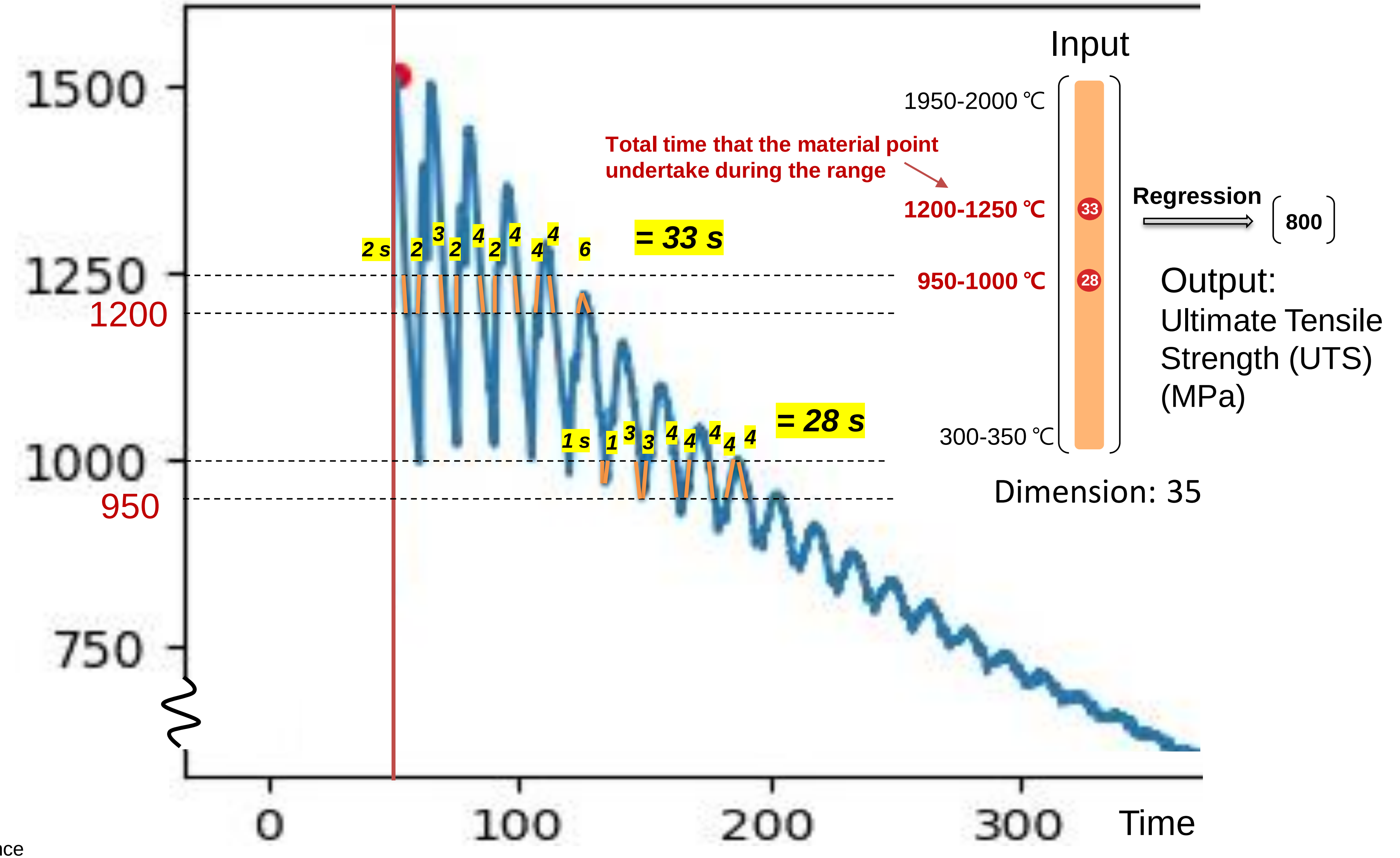

Different Regression Analyses are Performed with Segmented Data

Input: **reduced thermal history**

Output: **Ultimate Tensile Strength**

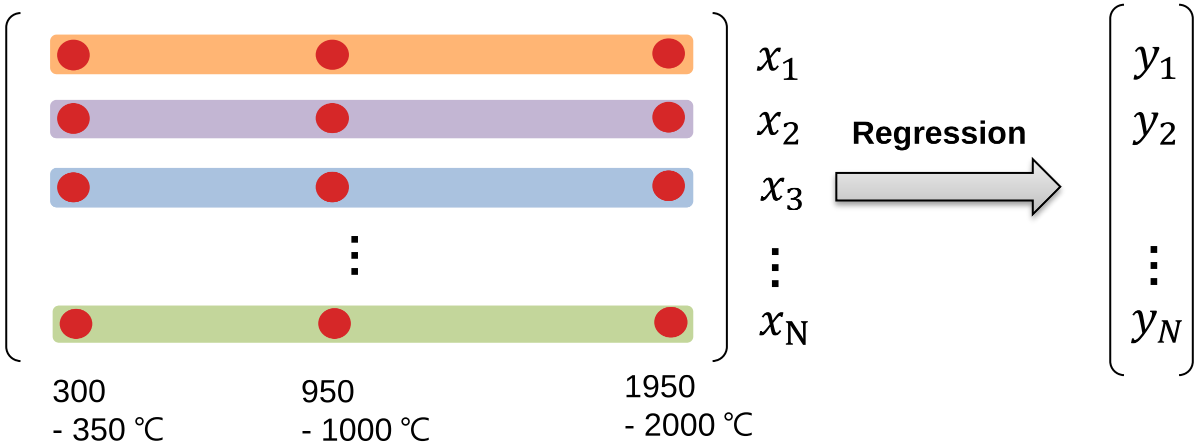

Dimension reduction:
17500 -> 35

N: the number of the training data

Randomly separate for 150 times:
Training data: 108 points (80%)
Test data: 27 point (20%)

Supervised learning algorithms:

- Least Squares Regression (LSR)
- Least Absolute Shrinkage and Selection Operator (LASSO)
- K-Nearest Neighbors (KNN)
- Support Vector Regression (SVR)
- Decision Tree (DT)
- Random Forest (RF)
- Gradient Boosting Regression (GBR)

Important Temperature Ranges Discovered by Random Forest Algorithm

Importance analysis via Random Forest - UTS

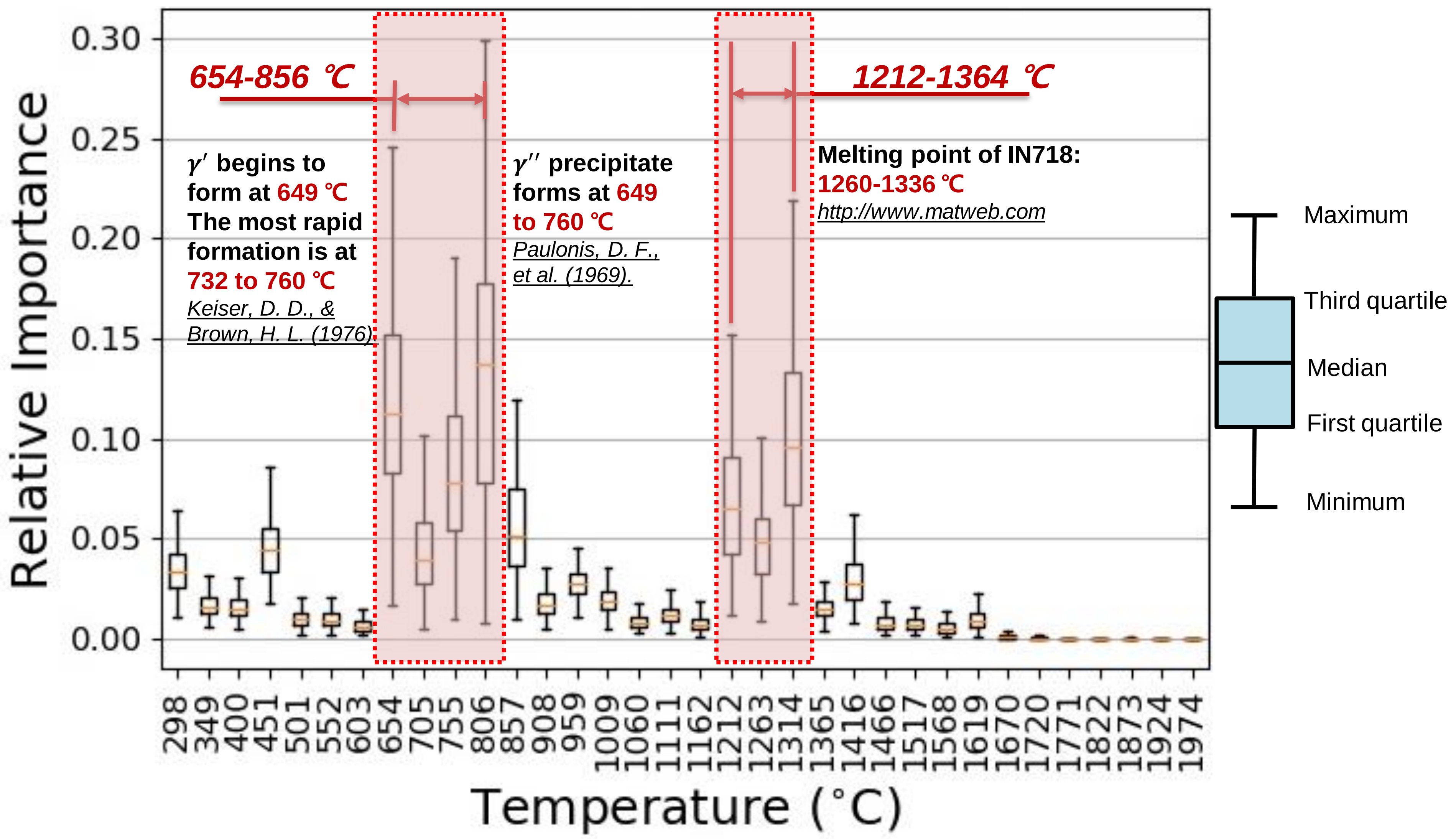

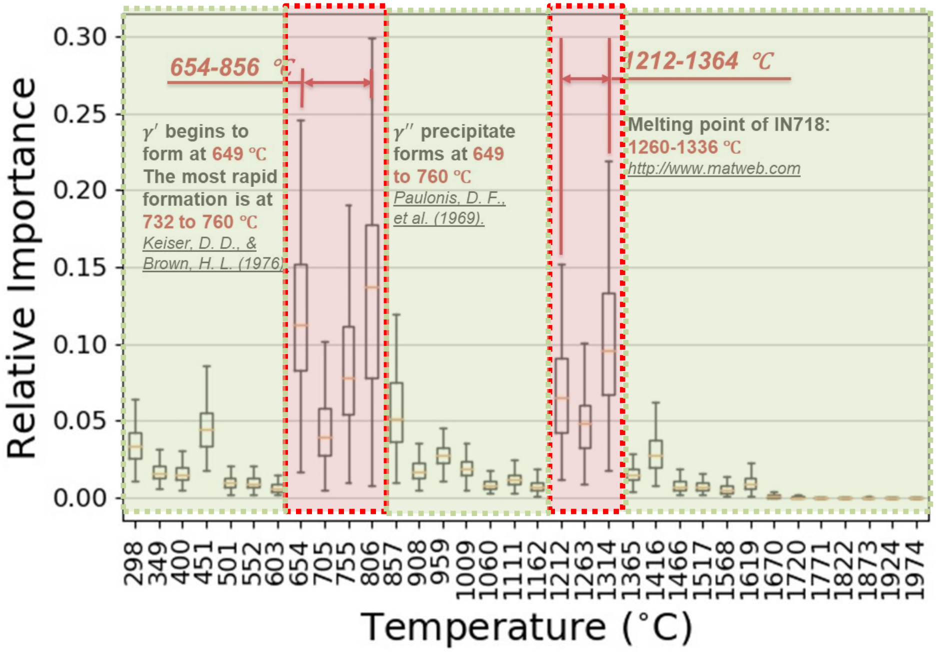

1. **Two dominant temperature ranges are identified without prior knowledge.**

2. **Solidification range: 1212-1364 ℃;**
   Solid-state phase transformation range: 654-856 ℃.

3. **Three temperature ranges: (a) higher than liquidus (1364 ℃) lower than 600 ℃ , and (c) between 856 ℃ and 1212 ℃ are not important notably for predicting UTS.**

4. **Only using solidification cooling rate is not enough for prediction of UTS in AM of Inconel 718.**

Using Linear Regression with Important Temperature Range Can Predict the Mechanical Response

Using three important intervals (1314-1365℃, 807-857 ℃, 654-705℃):

$$UTS = \underbrace{-9.63 * t_{1314}}_{\text{Negative effect}} + \underbrace{2.9 * t_{807}}_{\text{Positive effect}} + \underbrace{0.4 * t_{654}}_{\text{Positive effect}} + 758$$

Dimension: 17500 -> 35 -> 3

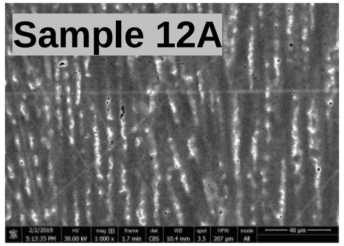

$t_{1314} = 5\ s$
PDAS $= 8.1\ \mu m$
$UTS = 1076.6\ MPa$

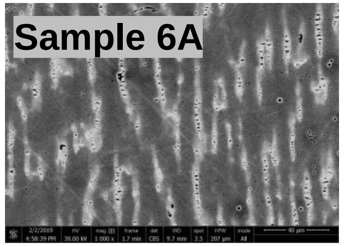

$t_{1314} = 7\ s$
PDAS $= 13.3\ \mu m$
$UTS = 884.7\ MPa$

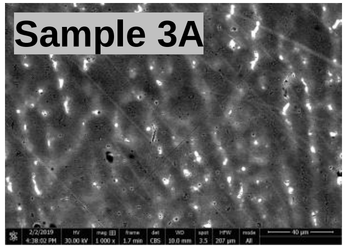

$t_{1314} = 10\ s$
PDAS $= 18.5\ \mu m$
$UTS = 649.4\ MPa$

*PDAS: primary dendrite arm spacing

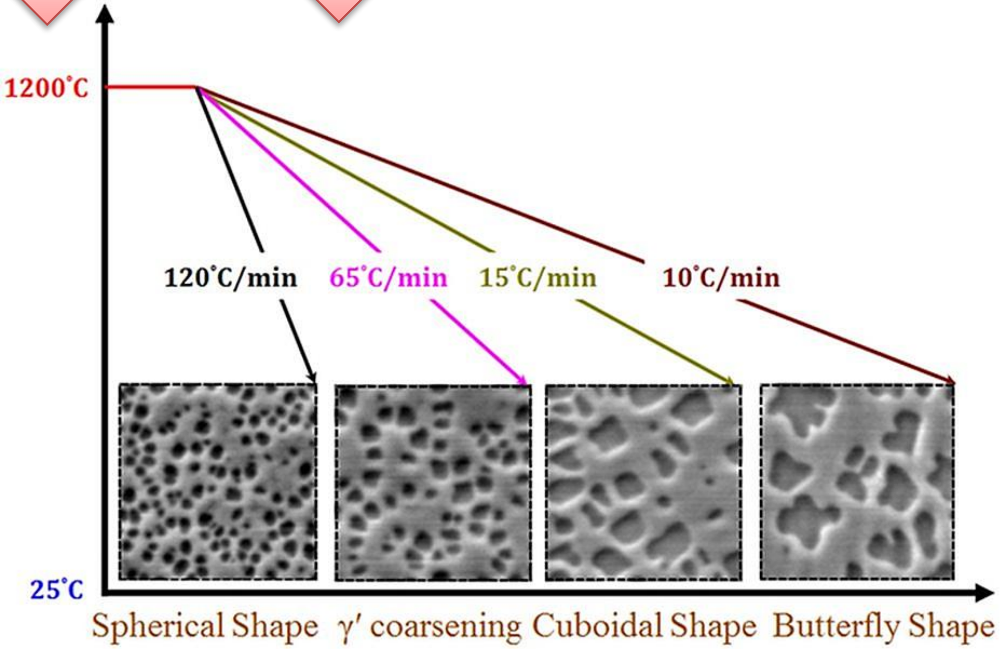

Masoumi, F., Shahriari, D., Jahazi, M., Cormier, J., & Devaux, A. (2016). Scientific reports, 6, 28650.

Increasing cooling time increases the volume fraction of γ'/γ'', strengthening the material

Correlative relationships between thermal histories and mechanical properties

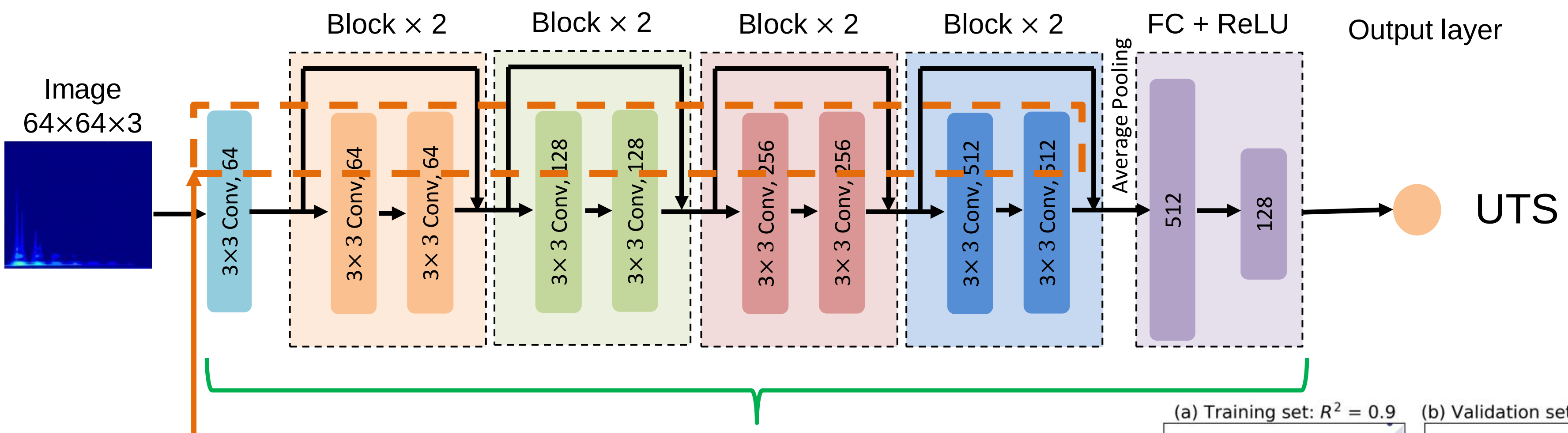

High-level mechanistic relationship is obtained by the hierarchical structure of CNN.

Different learnable filters can be used to capture different mechanistic features.

CNN maps well to from thermal histories to mechanical properties;

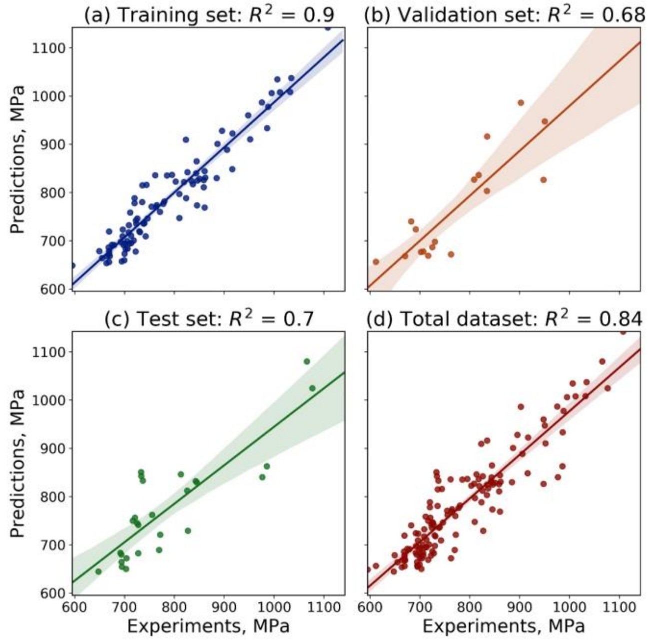

Data-driven prediction of UTS from thermal histories

- CNN predicted UTS (in black) and experimental values (in red) at marked locations.
- CNN can predict the UTS well when compared with experimental measurements.
- CNN model can be used to evaluate the weakest parts of the as-built thin walls.

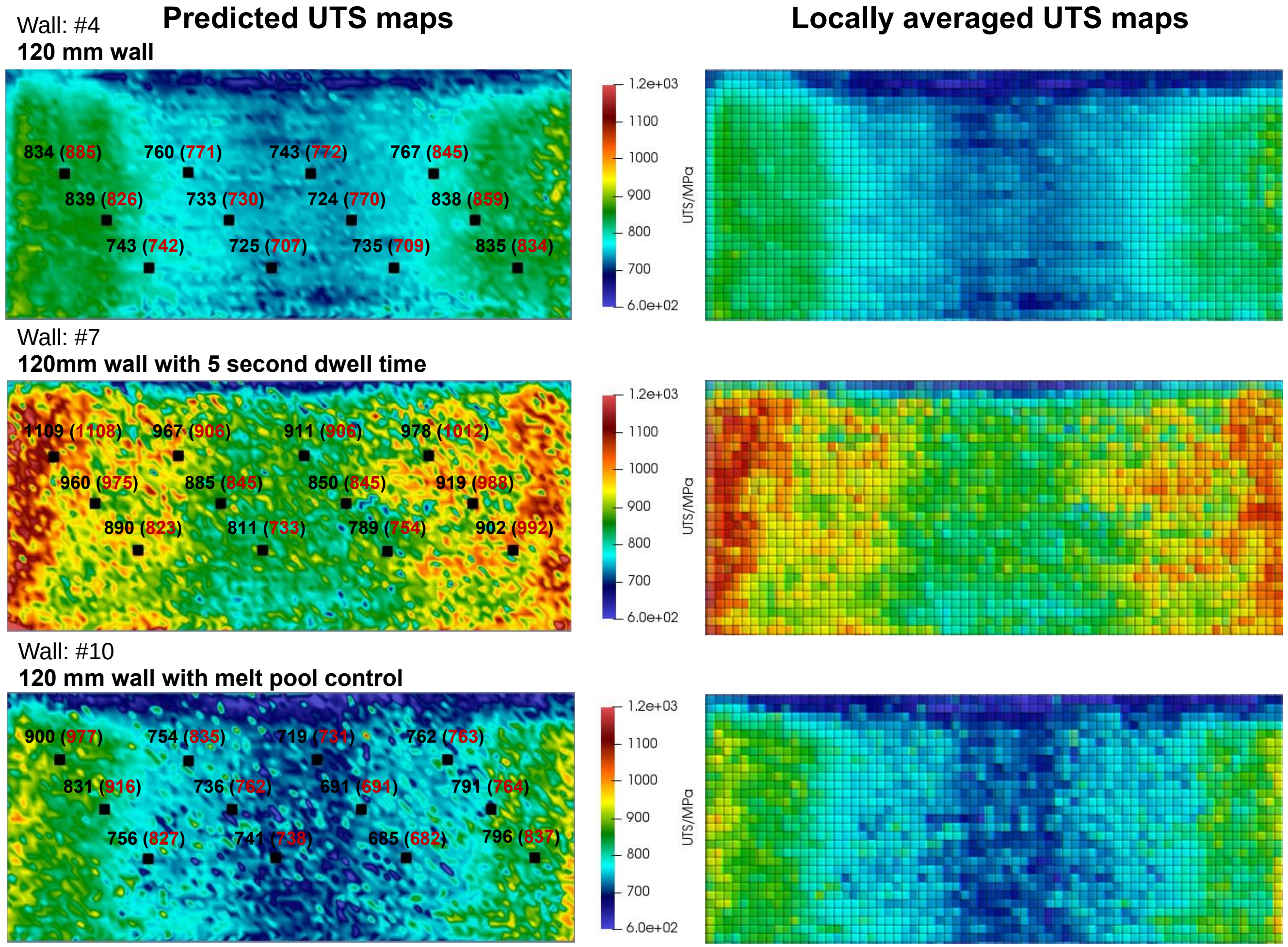

Standard deviation highly correlates with experimental observations of UTS in the training set

Standard deviation maps of predicted UTS

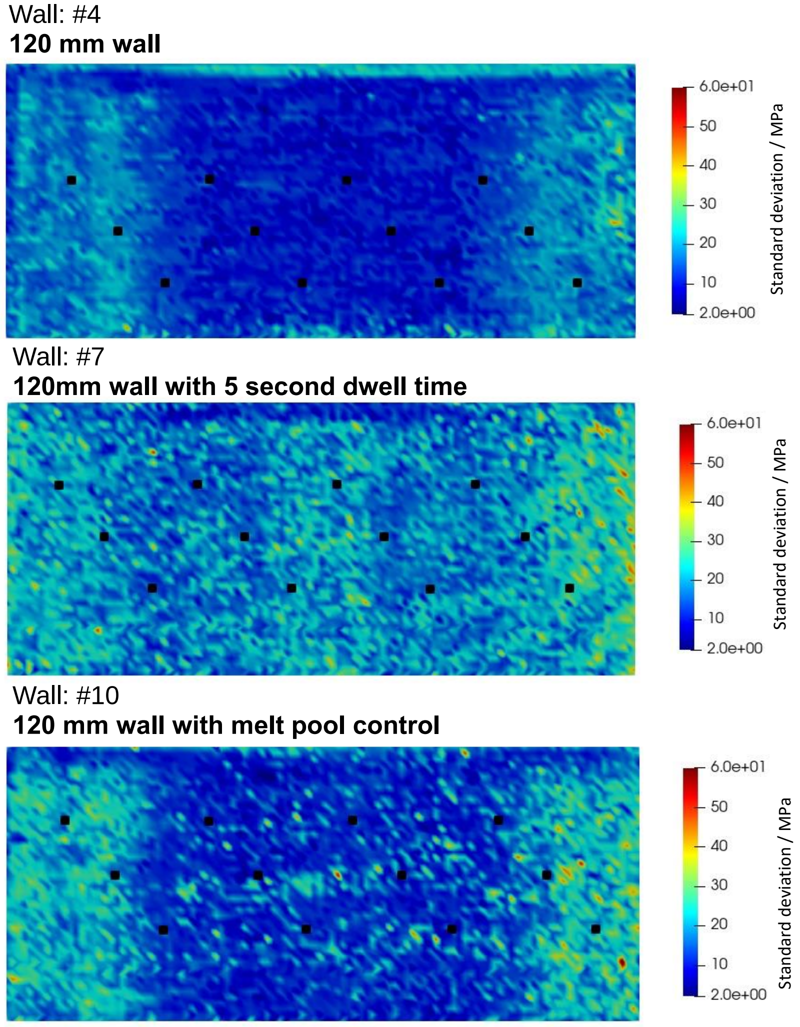

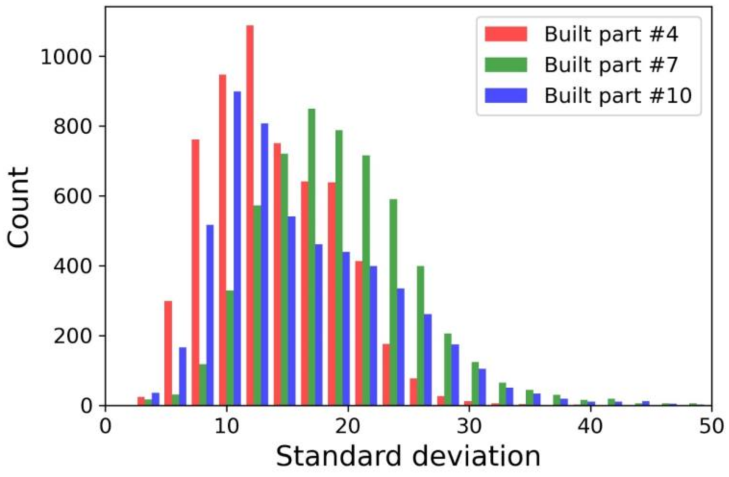

Standard Deviation Distribution for Predictions

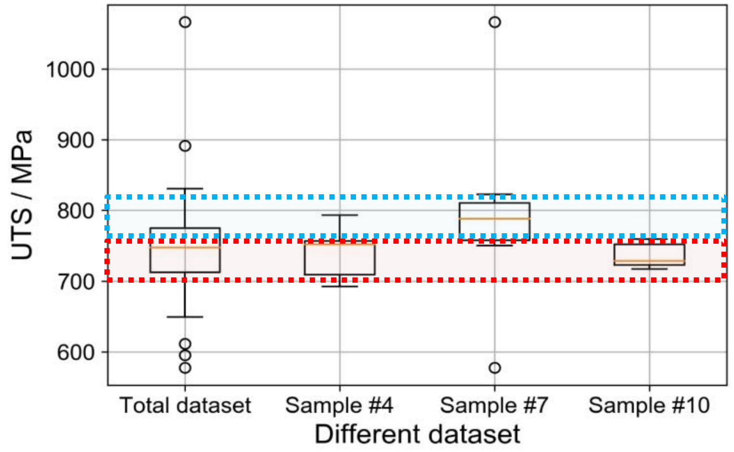

UTS (Exp. Data) distribution

Generalization to other mechanical properties

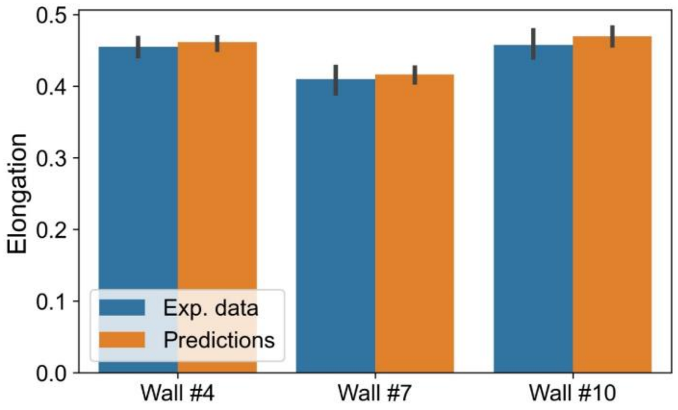

(a) Elongation

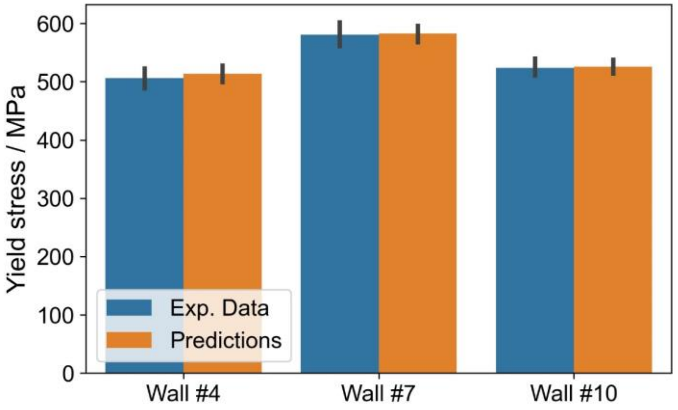

(b) Yield stress

Metrics	Statistics	Elongation			Yield Stress / MPa		
		Training set	Validation set	Test set	Training set	Validation set	Test set
R^2	Mean	0.7759	0.5428	0.4460	0.7719	0.6007	0.6791
	Std	0.0175	0.0671	0.0332	0.0914	0.0689	0.0546
MRE	Mean	0.0367	0.0489	0.0655	0.0488	0.0637	0.0556
	Std	0.0015	0.0043	0.0026	0.0132	0.0297	0.0046
MSE	Mean	0.0004	0.0008	0.0014	984.47	1567.90	1184.19
	Std	0.0000	0.0002	0.0001	465.25	1093.34	201.36
MAE	Mean	0.0166	0.0221	0.0295	22.6473	29.1507	27.6480
	Std	0.0008	0.0024	0.0013	5.1186	8.5509	1.9445

Note that for R^2, the higher the better. For MRE, MSE, and MAE, the lower the better.

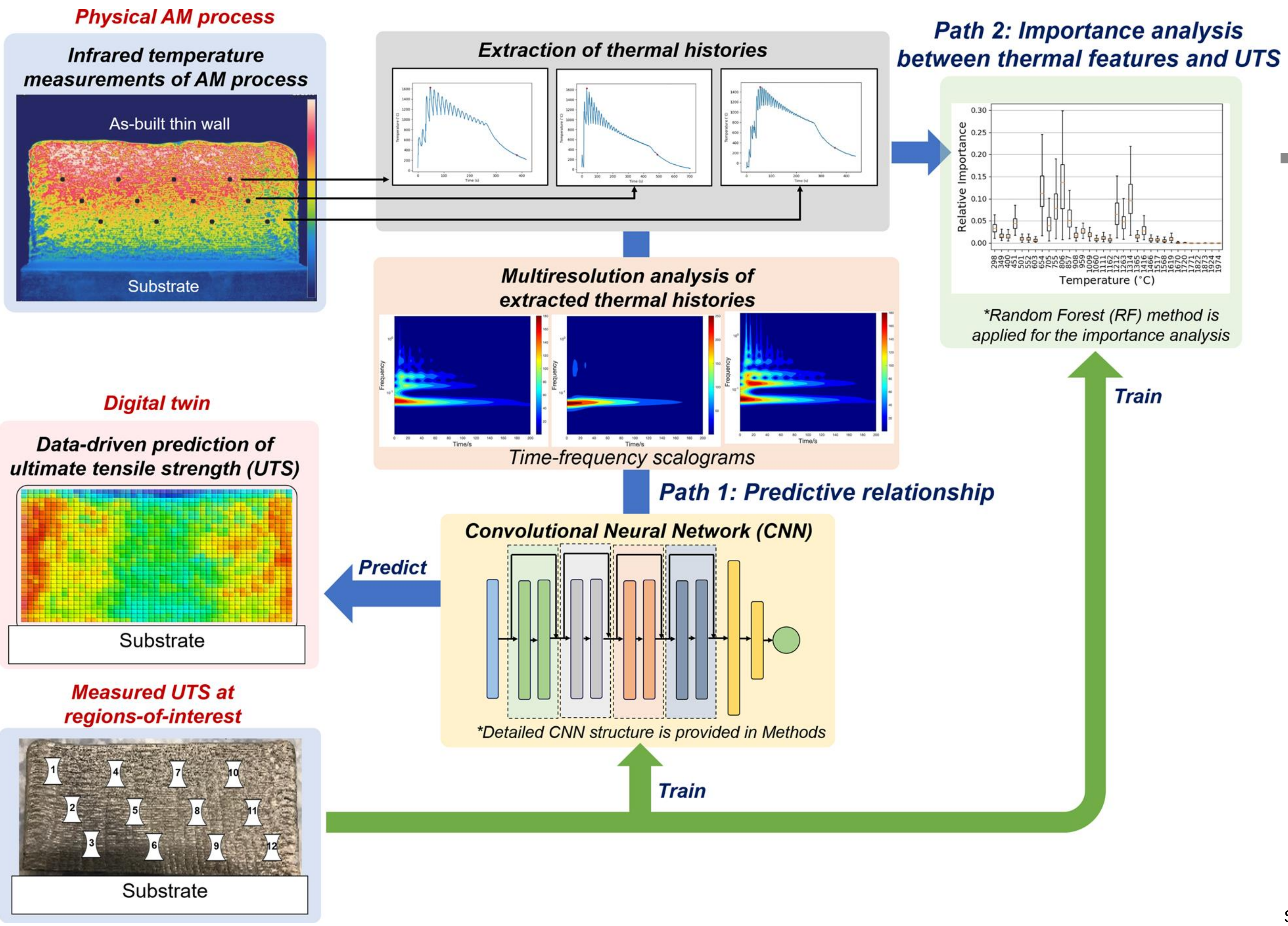
Physical AM process
Infrared temperature measurements of AM process
As-built thin wall
Substrate
Extraction of thermal histories
Path 2: Importance analysis between thermal features and UTS
Relative Importance
Temperature (°C)
*Random Forest (RF) method is applied for the importance analysis
Multiresolution analysis of extracted thermal histories
Frequency
Time/s
Time-frequency scalograms
Train
Digital twin
Data-driven prediction of ultimate tensile strength (UTS)
Substrate
Path 1: Predictive relationship
Convolutional Neural Network (CNN)
Predict
*Detailed CNN structure is provided in Methods
Measured UTS at regions-of-interest
1
2
3
4
5
6
7
8
9
10
11
12
Substrate
Train